

The Plasma Ion and Electron Instruments for the Genesis Mission

B.L. Barraclough¹, E. E. Dors¹, R.A. Abeyta¹, J.F. Alexander², F.P. Ameduri¹, J.R. Baldonado¹, S.J. Bame¹, P.J. Casey², G. Dirks², D.T. Everett¹, J.T. Gosling¹, K.M. Grace¹, D.R. Guerrero², J.D. Kolar¹, J.L. Kroesche Jr.³, W.L. Lockhart⁴, D.J. McComas¹, D.E. Mietz¹, J. Roesse², J. Sanders², J.T. Steinberg¹, R.L. Tokar¹, C. Urdiales², R.C. Wiens¹

¹Los Alamos National Laboratory, MS-D466, Los Alamos, NM 87545

²Southwest Research Institute, 6220 Culebra Rd., San Antonio, TX 78228

³Mobius Systems Corp, 15 S. Main St. #440, Logan, UT 84321

⁴Creative Circuitry, 1802 NE Loop 410 #15, San Antonio, TX 78217

Abstract

The Genesis Ion Monitor (GIM) and the Genesis Electron Monitor (GEM) provide 3-dimensional plasma measurements of the solar wind for the Genesis mission. These measurements are used onboard to determine the type of plasma that is flowing past the spacecraft and to configure the solar wind sample collection subsystems in real-time. Both GIM and GEM employ spherical-section electrostatic analyzers followed by channel electron multiplier (CEM) arrays for angle and energy/charge analysis and detection of incident ions and electrons. GIM is of a new design specific to Genesis mission requirements whereas the GEM sensor is an almost exact copy of the plasma electron sensors currently flying on the ACE and Ulysses spacecraft, albeit with new electronics and programming. Ions are detected at forty log-spaced energy levels between ~1 eV and 14 keV by eight CEM detectors, while electrons with energies between ~1 eV and 1.4 keV are measured at twenty log-spaced energy levels using seven CEMs. The spin of the spacecraft is used to sweep the fan-shaped fields-of-view of both instruments across all areas of the sky of interest, with ion measurements being taken forty times per spin and samples of the

electron population being taken twenty times per spin. Complete ion and electron energy spectra are measured every ~2.5 minutes (four spins of the spacecraft) with adequate energy and angular resolution to determine fully 3-dimensional ion and electron distribution functions. The GIM and GEM plasma measurements are principally used to enable the operational solar wind sample collection goals of the Genesis mission but they also provide a potentially very useful data set for studies of solar wind phenomena, especially if combined with other solar wind data sets from ACE, WIND, SOHO and Ulysses for multi-spacecraft investigations.

Introduction

The Genesis mission is the fifth in the NASA Discovery line of competitively selected, low-cost (<\$300M) missions designed to provide frequent access to space for mid-size planetary investigations that perform focused, high-quality science. The primary science goal of the Genesis mission is to precisely determine the average isotopic and elemental composition of the Sun and, by extension, the early solar nebula by returning pristine samples of the solar wind from space and performing detailed analyses of the samples using sophisticated, ground-based instrumentation. Laboratory analysis of the collected solar wind will yield results of much higher quality than is currently possible using spacecraft-borne instrumentation. See Burnett et al. (this issue) for a complete discussion of the Genesis science objectives.

The Genesis spacecraft (S/C) was launched on August 8, 2001 and is currently in a “potato-chip” halo orbit about the L1 point, located approximately 150 million kilometers sunward of the earth, where it is collecting solar wind ions into ultra-pure collector materials. The S/C is scheduled to make five, six-month orbits about L1 and then return to the vicinity of Earth in September of 2004. The Genesis Sample Return Capsule (SRC), a re-entry vehicle containing all of the solar wind samples, will separate from the spacecraft

and then make a direct entry into the earth's atmosphere above Utah. The SRC will be slowed by deployment of a parafoil and then captured in mid-air by helicopter. Subsequently, the samples will be taken to clean room facilities for sample curation and eventual analysis. These will be the first samples returned to Earth from space since the last lunar samples were returned in the early 1970's during the Apollo program. A large fraction of the returned samples will be archived for study in the future when currently unknown analytical techniques and instrumentation may become available.

The entire science payload of the Genesis spacecraft consists of the plasma ion and electron spectrometers, the subject of this paper, the solar wind Concentrator (Nordholt et al., this issue), which concentrates solar wind ions by ~20X into ultrapure collector materials (Wiens et al., this issue), and various passive collector materials described in detail by Jurewicz et al. (this issue). While not a hardware item, the WIND algorithm is also considered to be part of the science payload. This code, which resides in the S/C Command and Data Handling (C&DH) subsystem, uses data from the plasma spectrometers to make real-time decisions about the type of solar wind flowing past the spacecraft and adjust the active sample collection subsystems appropriately (Neugebauer et al., this issue).

The Genesis S/C consists basically of a thin, honeycomb equipment deck with the SRC, plasma instruments, solar panels and numerous other subsystems attached (Figure 1). It is spin stabilized during normal operation at 1.6 ± 0.16 rpm with the +X spin axis pointing 4.5 ± 1.0 degrees ahead of the sun, which is the average, aberrated solar wind direction at L1. This orientation was dictated by the Concentrator pointing requirements, which are discussed in a companion paper (Wiens et al, this issue). The electron and ion spectrometers, collectively referred to as the Monitors, are located on the S/C deck at clock angles of 45 degrees (GEM) and 225 (GIM) degrees relative to the +Y axis (Fig. 2). The S/C spins about the X-axis in a counter-clockwise direction when viewed from the Sun. Magnetic fields generated by the S/C have been controlled such that any electron entering the electron spectrometer aperture will encounter no more than a 600 nT field along its path.

The use of suitable multi-layer insulation (MLI) blankets limits electrostatic potentials to <50 mV within 0.5 m of either Monitor entrance aperture and to <2.0 V anywhere on the S/C, except for specially waived locations/items.

Requirements for the Plasma Spectrometers

Genesis is a somewhat unique mission in that the science phase doesn't formally begin until the flight portion of the mission is concluded and the solar wind samples have been distributed to ground-based laboratories for analysis. Despite the inclusion of plasma instrumentation in the science payload, there are no formal science goals/requirements for the Monitors as would be the case for a traditional heliospheric, magnetospheric or other space physics mission. Rather, the plasma instrumentation is present solely to support the collection of the solar wind samples and so, in this case, functions more as a S/C subsystem than as a science investigation. No provision was made to accommodate a magnetometer, an energetic particle investigation, a radio wave experiment, etc., as these were determined to be not strictly necessary to support sample collection. While solar wind studies are not primary science goals for Genesis, some very useful space physics can be done with the limited instrumentation available on Genesis.

The plasma spectrometers and WIND algorithm are tasked with enabling the collection of two types of solar wind samples during the course of the Genesis mission. The first type is referred to as "bulk" sample where collector materials are continuously exposed to the solar wind without regard to the type or origin of the flow to which they are being exposed. The main operational requirement for collecting this type of sample is that the S/C pointing is controlled within certain limits. The Concentrator, which is an *active* bulk-sample collector, additionally requires knowledge of the solar wind flow speed and temperature so that its collection efficiency can be continually optimized for varying solar wind conditions by adjustment of the internal ion-optics.

The second type of solar wind sample to be collected is the “regime-specific” sample where a given passive collector is exposed to the solar wind flow only when a specific type of solar wind is flowing past the S/C. These regime-specific solar wind samples are being collected in order to elucidate any elemental and isotopic variations that may exist in three types of solar wind flows. The three solar wind regimes are 1) fast and fairly uniform solar wind emanating from coronal holes, 2) slower and more variable solar wind originating in the streamer belt, and 3) material being carried from the solar atmosphere in coronal mass ejections (CMEs). Analysis indicates that the minimum set of parameters that needs to be known onboard to reliably distinguish among the three regimes include solar wind proton speed, temperature and density, alpha particle abundance, and the presence or absence of bi-directional electron streams. It is the measurement and interpretation of these five parameters that are the primary operational requirements for the Monitors and the WIND algorithm. The paper by Neugebauer et al. (this issue) describes how the Monitor measurements are used to determine the solar wind regime and control the active collector subsystems, namely the Concentrator and the Collector Arrays, in real-time.

In contrast to many other missions, there were no particularly severe weight, power or volume constraints for the Monitors and consequently there were no extraordinary efforts taken to minimize use of these resources. Radiation hardness requirements were minimal with a total anticipated dose over the course of the mission of only 12 krad behind 60 mils of aluminum. Early in the mission design phase, there were tight telemetry constraints (~400 bps for both Monitors) and instrument operations were consequently designed to measure complete ion and electron energy spectra at the relatively slow cadence of once every 2.5 minutes. Much later, these requirements were relaxed considerably after a redesign of the downlink strategy but by then design, fabrication and coding were too far advanced to modify the Monitor operating scheme and take advantage of the increased telemetry rate available, with the result that the relatively slow temporal resolution of the Monitors was carried forward.

The Genesis Ion Monitor (GIM)

The GIM plasma ion spectrometer consists of a spherical-section electrostatic analyzer (ESA) for energy and angle analysis of incoming ions, followed by a custom array of Dr. Sjuts Optotechnik channel electron multipliers (CEMs) for single-ion detection (Fig. 3). The ESA has a 120-degree bending angle, a central radius of 60 mm, a nominal analyzer gap of 1.8 mm and an entrance aperture with dimensions of 1.8 x 2.9 mm (Table 1). For UV rejection, the ESA plates have been copper coated and blackened with an Ebanol-C coating and the inner surfaces have been grooved transverse to the ion trajectories. These 0.79 mm radius grooves (0.13 mm deep with 0.84° period) have the effect of changing the effective electrostatic radii of the inner and outer analyzer plates, decreasing the analyzer constant, $k = \text{accepted energy divided by ESA voltage}$, from an ideal value of 16.7 to a calibrated value of 14.7. The ESA electrical configuration has the inner plate biased with a stepped, negative high-voltage while the outer plate is held at ground potential thus steering ions of appropriate energy/charge (e/q) into the CEM detectors. The analyzer k and the ESA high-voltage power supply (HVPS) range define the 1 eV to 13.6 keV energy range of the sensor.

The CEM detector array consists of eight individual CEMs, each with a rectangular entrance funnel of 2.75 x 10.0 mm. The height of the CEMs is such that all ions exiting the curved ESA gap will be intercepted by the array, while the width and placement of each CEM was selected to obtain the desired polar angular response of the instrument. The electrical biasing scheme for the CEM array is as follows. A negative high-voltage potential (0 to -4.0 kV, -2.5 kV typical) is applied to a secondary-electron suppression grid (~90% transmission) that is mounted directly in front of the CEM funnels. This has the effect of post-accelerating analyzed ions by the amount of the applied potential. A resistor is used to drop ~ 50 V between the screen and the CEM funnels and this further accelerates the

incoming ions and also pushes secondary electrons liberated by the impacting ions back toward the funnel thereby increasing detection efficiency. The CEM channel exit is held at $\sim +50$ V relative to ground such that the exiting charge cloud is efficiently pulled across a small gap to the anodes that are at ground potential. The CEMs have a nominal gain of $\sim 1 \times 10^8$ at 2300 V and a 3 kHz counting rate. Charge pulses collected at the signal anodes are routed to Amptek A121 hybrid preamplifiers in the front-end electronics (FEE). The resulting digital pulses are accumulated in 16-bit scalers until they are read out to the S/C C&DH subsystem. The preamplifiers have a fixed deadtime of 0.5 μsec .

Mechanically, the ESA/CEM assembly is mounted in a “coffin” that hermetically isolates the sensor interior from contaminants while on the ground (Fig. 4). A single-use aperture door mechanism, actuated by redundant Eagle-Picher dimple motors, is used to open the aperture door in flight. Pumping of the coffin volume to space is achieved via a blackened pump-out baffle box and to a lesser extent via the particle entrance aperture. As the GIM aperture stares at an angle quite close to the sun, special care was taken to baffle the area around the aperture to prevent stray light from producing any unwanted background in the detectors.

The sensor coffin is mounted on a wedge-shaped interface piece that is located between the coffin and the Monitor Electronics Box (MEB), which interfaces to the S/C deck and electrical subsystems. The wedge serves as a housing for the FEE and this piece is also used to position the GIM field-of-view (FOV) relative to the S/C spin axis. As each CEM has a pixel size of $\sim 3 \times 4$ degrees, the overall GIM FOV is a narrow fan with dimensions 4×26 degrees (Fig. 5). The 10.5 degree tilt of the wedge orients GIM such that the center of the FOV of CEM #1 is parallel with the S/C spin axis (i.e. the edge of the viewing fan overlaps the spin axis by ~ 1.5 degrees).

The Monitor Electronics Box (MEB) is the main electronics component of both the GEM and GEM instruments and is of new design specific to the Genesis mission requirements. The unit accepts commands from the spacecraft to initiate sensor data

collection and control the HVPSs. For cost-saving purposes, the MEBs for both GIM and GEM were designed to be nearly identical. (It should be noted that the redundant Concentrator Electronics Boxes (CEBs) for the Concentrator are also almost identical to the MEBs, but these are not discussed here). The primary difference between the units is the polarity and range of the output power supplies (Table 2). Each MEB has external dimensions of 5.1 x 16.5 x 21.6 cm (2 x 6.5 x 8.5 in.), weighs ~1.4 kg, consumes ~4W, and contains separate controller and HVPS printed circuit boards. The boards are partitioned for a) HVPS analog electronics (HVPS) and b) microcontroller logic/analog I/O circuits (controller).

The controller board is based on a radiation-hardened UT80C196KD micro-controller operating at 12MHz, with the following resources:

- 16 kBytes of PROM
- 32 kBytes of SRAM
- 12-bit DACs (power supplies have 4096 commandable levels)
- 8-channel multiplexed 12-bit ADC
- 1 and 100 kHz test pulser (for signal electronics chain verification)
- 16-bit scalers for FEE pulses
- Discrete inputs (enable and limit)
- Discrete read backs (enable and limit)
- 19.2 kbps full duplex serial port (RS422)
- +5V and +/-12V power supply custom dc to dc converter
- EMI filter and redundant power input OR diodes

Each MEB controller contains firmware stored in radiation-hardened PROM to customize its function for either GEM or GIM. Built-in test features allow verification of ADC, DAC, counter, FEE, and spacecraft interface functions. Analog commands sent from

the controller to the HVPS are looped back into the ADC multiplexer for comparison of commanded values to voltage monitor read backs.

The HVPS boards are based on a resonant flyback converter topology, operating at ~100kHz. Each power supply is scaled to accept a 0 - 5V analog command from the controller. Each output returns a 0 - 5V scaled output voltage monitor that is digitized and inserted into telemetry by the controller. A safety interface is provided for ground operations via an external connector. Limit and enable discrete inputs are provided at this connector in parallel with the open-collector outputs from the controller board. "Limit" sets the output voltage to ~10% of the commanded value. "Enable" is used to turn the outputs on and off. This connector is covered for flight configuration. For safety, all power supplies are designed to operate into a short circuit indefinitely without damage.

GIM Response and Calibration

The response of the ion spectrometer was determined by illuminating the sensor entrance aperture with a uniform, monoenergetic ion beam and recording the count rate of each of the eight CEM detectors for all combinations of ESA voltage, azimuthal angle and polar angle to which the instrument is responsive. In this manner, a 3-dimensional array of transmission values, as a function of azimuth angle, polar angle and ESA potential (equivalent to incident ion energy/charge, e/q) was built up for each detector. The response function of the GIM can be completely determined using these eight data cubes. The relative responses of the GIM were calibrated to absolute beam flux using a solid-state detector with known output as a function of beam current.

Some of the results of the GIM calibration can be seen in Figure 6 and 7. The response shown in all of the 2-dimensional plots has been integrated over the energy-angle variables that are not shown. For instance, the polar vs. azimuthal response shown in Fig. 7a has been integrated over energy, while the polar vs. transmission plot in Fig. 7b has been integrated over energy and azimuth.

The energy response of the GIM ESA is shown in Fig. 6. The transmission curves have been integrated over polar and azimuth angle and have been normalized to the maximum count rate observed for all CEMS. It can be seen that the integrated energy resolution is ~5.2% FWHM, which corresponds well with the 5.0% design value. The plot shows a slight variation in the central energy for the different CEMs, probably due to a small misalignment of the ESA hemispheres and/or a drift of the beam energy during the calibration. The integrated transmission amplitudes vary by as much as $\pm 8\%$ across the eight detectors. There is a small cosine effect that causes transmission to drop with increasing polar angle (aperture area effect) but this is not sufficient to cause all the variation observed. Probable causes of additional amplitude variation in the individual responses include variability in CEM absolute efficiency, slightly varying CEM funnel widths and drift in the beam current during calibration.

Figure 7a shows the response “islands” of the eight-member GIM CEM array, integrated over energy and normalized to the maximum transmission for each detector. Plotted contour levels are for 90, 75, 50 and 25% response levels. The FWHM of the overall GIM viewing fan is approximately 4×26 degrees with the central response of each CEM being spaced at ~3 degrees as desired. Fig 7b illustrates the GEM polar angular response integrated over energy and azimuth angle. Note that there is a very slight deviation of the response maxima from the nominal three degree CEM-to-CEM spacing due to manufacturing tolerances in the funnel widths. It can also be seen that there are no gaps in the polar angular coverage due to the very good overlap of the CEM responses at the 50% transmission level. The azimuthal angular response of the GIM is shown in Fig. 7c. The response curves have been integrated over energy and polar angle and the responses have been normalized to the highest transmission value observed. An integrated azimuthal resolution of ~4.2% FWHM can be extracted from the curves. The ~1.5 degree azimuthal offset of the central response in can be attributed to the effect of fringing fields present near the entrance aperture and/or a small misalignment of the sensor in the calibration chamber.

The GIM calibration data show that the sensor meets all design goals and that there is good angular coverage of the sky with no gaps in energy or angular response. As the GIM viewing fan sweeps out a circle of ~25 degree radius centered on the average, aberrated solar wind direction, GIM will adequately capture the solar wind beam distribution over the bulk of the mission

GIM Operation

During normal operation, the Genesis S/C spins at a nominal rate of 1.6 ± 0.16 rpm and, due to telemetry restrictions, four spins of the S/C (nominally 2.5 min) are used to generate complete ion and electron spectra. These four spins of data collection are referred to as a complete data cycle. The operation of both Monitors is synchronized to the spin phase of the S/C and both Monitors are forced to start a data cycle and subsequently acquire data in tandem such that if the GIM is in the second of a four-spin data cycle, the GEM must also be in the second spin. If, due to various problems with data acquisition, one of the Monitors calls for a repeat of a spin, the other Monitor must also perform a spin repeat. Both Monitors start their spins at the same time, which means that the sensor viewing fans are always 180 degrees out of phase as the Monitors are mounted on opposite sides of the S/C (Fig.2).

The Attitude Control System (ACS) continually determines (among other things) the spin rate and spin phase of the S/C via star-tracker data that updates at a nominal rate of ~1.6 Hz. The S/C spin axis lies in the ecliptic plane pointing slightly to the west of the Sun. The spin phase zero azimuth for the S/C has been defined as when the center of the GEM FOV is aligned with the north ecliptic normal. At each spin phase zero crossing, ACS sends a synchronization, or “sync” pulse to both Monitors with an accuracy of ± 10 msec. (~0.1 deg. of roll). As soon as the sync pulse is received, both Monitors act on a command that is already present in their command buffers and begin a new spin of operation. In the event

that the ACS can't accurately determine when to send the sync pulse, a synthetic sync pulse appropriate for an exact spin rate of 1.6 rpm is continuously sent until ACS recovers. Knowledge of the S/C spin rate is also used by flight software (FSW) to continuously expand and contract (within $\pm 10\%$ limits) the length of the data acquisition cycle for each spin as the spin rate of the S/C varies during the mission. This is accomplished by calculating the exact energy step-time (see below) needed for each spin so that the data acquisition cycle completely fills each spin period and all phase space samples remain aligned in look direction.

The GIM has two basic operating modes: Normal and Manual. The Normal mode has two different submodes, Search and Track, which are very similar and differ mainly in the scanned energy range. A variant of the Manual mode is the Calibrate (Cal) mode where several Manual configuration commands are sequenced to perform a CEM gain measurement.

In Manual mode, a configuration command is sent to GIM, the sync pulse arrives and initiates the reconfiguration of the sensor, and the state of the sensor remains static until a subsequent command is received. This mode is useful for instrument turn-on/off, troubleshooting, periodic maintenance and CEM gain calibration. A Manual mode configuration command is used to set: fixed HV levels for the CEMs and the ESA, the discriminator voltage level, the integration, settle and step times (see below) and test pulser off/on.

GIM Calibration mode is simply a fixed sequence of Manual mode acquisition commands that is used to calibrate the gain of the CEM detectors. Basically, the ESA potential and discriminator threshold levels are held at fixed values for the entire five-spin Cal cycle while the CEM HVPS is fixed at different values for each of the five spins. Cal mode must be entered directly from normal mode as the energy level of the proton peak from the last normal mode data cycle is needed to select the fixed ESA voltage level that will be used for the Cal cycle.

GIM Cal mode starts by determining the ESA level that gives the peak counting rate for the current solar wind conditions and fixing the ESA at this energy level for the next five spins of the S/C. The CEM HVPS is then set at a different value for each of the next five spins in the sequence -2 , -1 , $+1$, $+2$, $+0$, where Δ is a configurable number but is typically 100V. GIM completes the Cal cycle and then returns to normal mode in its previous configuration. Data from the five CEM settings can now be evaluated to determine if the CEM gains need to be adjusted at a later date. An option exists to systematically vary the level of the discriminator threshold during a Cal cycle to determine if the current settings are appropriate. If this option is selected, the threshold voltage is stepped in the sequence -2 , -1 , $+0$, $+1$, $+2$ (Δ is configurable but typically ~ 0.3 V) at the same cadence as energy stepping occurs during normal mode operation.

As the name implies, GIM Normal mode is the operating cycle that will be used during the bulk of the mission. During standard operation, a complete ion spectrum is generated every four spins of the S/C. For each spin, GIM acquires particle counts from eight CEM detectors at ten log-spaced energies in each of forty azimuthal directions. Each of the four spins uses a different set of ten energies such that at the end of every data cycle the sensor will have acquired a data matrix consisting of detector counts from eight polar angles (set by CEM look direction), forty azimuthal angles (determined by S/C spin-phase) and forty energy levels (10 levels/spin x 4 spins/cycle).

Figure 8 shows a schematic view of a complete four-spin Normal mode data cycle. Energy stepping within a given ten-step sweep is always from high to low except for voltage flybacks and the ten energy levels used for a given spin are always higher than those used for the subsequent spin except when a new data cycle is initiated. A complete ten-step energy sweep takes slightly less than a second and depends on S/C spin rate.

Figure 9 shows some of the details of individual energy steps. The steps are log-spaced in voltage (energy) with a typical value being 5.26% spacing between steps. First, a settle time is specified that allows the HVPS to stabilize at the new voltage setting. This

number is configurable over a wide range by Manual mode command but is typically held at 10 msec. When the settle time expires, integration time (also set by Manual mode command) begins and ion counts are accumulated in the scalers for the specified period, typically 40 msec. This number is decreased if counter spills are routinely encountered or increased if improved counting statistics are desired. At the expiration of the integration time, slack time begins. This period is not fixed and dynamically varies depending on S/C spin rate and specified settling and integration times such that :

$$\text{Slack time} = \text{Step time} - (\text{Settling time} + \text{Integration time})$$

Step time is specified by FSW at the beginning of each spin as will be seen below. As soon as slack time begins, the internal microcontroller sends the ESA HVPS to the next of the ten voltage levels so that the power supply actually has slack time plus settle time to stabilize. In certain situations, slack time can decrease to zero and in this case the HVPS will at least have the fixed integration time to settle.

A Normal mode data acquisition cycle is initiated as follows. FSW is aware of the S/C spin rate and calculates the spin period for the upcoming spin. Using this information, the step time required for the 400 energy steps (40 spin sectors x 10 energy steps/sector) to completely fill the upcoming spin time is calculated. The starting level of the first voltage step is also determined (see below) as is the step size. Step size is configurable and changes depending on whether GIM is in Search or Track submode. These three parameters (step time, start level and step size) are calculated by FSW and sent to the GIM at any time between one and ten seconds before the next sync pulse is anticipated. The values are then stored in the GIM command buffer and are then passed to the microcontroller as soon as the sync pulse arrives at which time the processor then initiates the data acquisition sequence for the next spin.

The GIM ESA HVPS has a 12-bit (4096 level) control that can linearly step the energy acceptance of the GIM from 0 to 13.7 keV. During any given data cycle however, only forty logarithmically-spaced steps will be utilized and these steps shift in energy from

data cycle to data cycle as the flow velocity of the solar wind varies with time. It is desirable to keep the solar wind proton peak centered appropriately in the energy sweep such that protons, alpha particles and higher e/q species are adequately covered even as the speed and temperature of the beam varies. This is accomplished by employing a Track submode wherein the peak count rate in the previous data cycle is used to fix the scanned energy range of the subsequent data cycle. Given a forty-level energy sweep at 5.26% spacing, an attempt is made to always have the peak count rate (i.e. the proton peak) fall in level 28 (eighth step of spin#3), which will insure that no significant portion of the proton distribution at low energies will be missed and that the high-energy tail of the alpha distribution will be adequately covered even when the beam is hot. Once the peak count rate of a given data cycle is found in energy, FSW calculates what the voltage start level of the next cycle should be to keep the peak rate in level 28. This initial start level is used by FSW to calculate the other three different start levels for each of the other spins of the data cycles. When GIM receives the acquisition command from FSW to begin each new spin, the internal microprocessor uses the start level and step size to calculate the set of ten voltage steps to be used for a particular spin.

It is conceivable that the energy of the solar wind beam might shift sufficiently between the start of consecutive data cycles to cause the proton peak to fall outside of the scanned energy range. In this case, the software might lock onto the alpha peak and track this feature for some time, missing the proton peak completely and generating bad measurements that would confuse the WIND algorithm. To address this problem, a Search submode has been implemented where once every 25 track cycles (the number is ground configurable), the range of the energy sweep is doubled from its normal 8X to 16X by changing the voltage step size. A fixed start level is always employed for Search, i.e. the energy range does not vary with solar wind conditions. The Search submode insures that GIM will never track a false peak for more than about 30 minutes, in the remote case that the proton peak jumps outside the energy range scanned in Track submode.

GIM Data

All data acquired by GIM during a data cycle are used for onboard moments calculations while only a subset of the data selected by a masking algorithm (see below) is telemetered to the ground. Prior to being inserted into the telemetry stream, the GIM counts data are compressed from 16-bit to 8-bit numbers using an algorithm that introduces a maximum of 3% error in the transmitted counts. The combination of masking and data compression reduces the effective science data rate of the GIM from ~1365 bps of data sent from GIM to the C&DH subsystem to ~169 bps sent to the ground. GIM data are corrected onboard, prior to being used for moments calculations, for electronic deadtime and for background in the detectors. The background correction involves use of an algorithm that finds the polar and azimuthal angle of the center of the solar wind beam and then finds the azimuth that is 180 degrees opposite. Counts data at this location for CEM#8 at the two highest energy levels are then averaged with that from the two nearest azimuthal neighbors to get a six-number background counts average. If the average is <10 counts, no correction is made. For a background count average between 10 and 500, the correction is subtracted from each data element before further processing. If the average exceeds 500 counts (background count rate ~12.5 kHz) the GIM data is marked false and onboard moments processing is suspended until background rates subside.

The GIM data sampling sequence described above, in concert with the detector mounting geometry, effectively produces an over-sampling of that phase space containing the solar wind ions. In addition, the sampling sequence typically makes measurements in directions well off the solar wind beam direction. In order to reduce the amount of GIM data included in the downlinked telemetry, a masking algorithm is applied which dynamically chooses a subset of the GIM counts samples for transmission. The mask

eliminates counts samples at look directions that are highly overlapping, or are at angles far away from the direction of the peak ion flux.

At each of the forty energy levels used, the GIM accumulates particle counts in all eight CEMs at forty different satellite spin azimuth positions. The samples from eight CEMs and 40 spin azimuth angles comprise a sample space of 320 phase space look directions. The masking algorithm selects 80 of those 320 phase look directions for downlink. As the spacecraft rotates, CEM#1 takes forty samples, all over-lapping in phase space. Samples from other CEMs with FOV closer to the spin axis direction are more heavily over-sampled than those with FOV directed further from the spin axis direction. On a given data cycle, the masking algorithm takes into account the CEM and the spin azimuth angle for which the highest counts were recorded, i.e. the location of the solar wind beam. The peak-counts CEM and together define a peak sample look direction. A subset of minimally overlapping samples is chosen which are concentrated within 12 degrees of the peak sample look direction, but have some sample coverage out to approximately 18 degrees from the peak sample look direction.

Figures 10a and 10b show examples of what is meant by masking. On a polar projection, pluses indicate the look directions for the 320 samples collected onboard for each data cycle. Diamonds are plotted over the pluses to show the masked data chosen for downlink. Figure 10a shows the case where the peak counts were found in the CEM closest to the spin axis. Figure 10b shows an example in which the peak counts were found two CEMs away. When flight software determines that the CEM and azimuth with the peak counts cannot be definitively chosen, GIM defaults to the mask centered on the most spin axis aligned CEM, shown in Figure 10a,.

There are two additional data “modes” that are available for use and these can be selected from the ground when required. These modes were primarily used for system-level testing prior to launch but will also be invaluable should problems be encountered in flight. The first mode is called “diagnostic mode” and the main difference between this data

stream and normal GIM telemetry is that the mask is not applied to the telemetered data before transmission, i.e. all 320 phase space samples are telemetered, not just the 80 normally selected by the mask. This increases the GIM telemetry rate by a factor of four from the normal rate and so must be used only when adequate onboard storage and/or downlink time is available. There is no comparable diagnostic telemetry mode for GEM as no masking scheme is employed with the data from this instrument.

The second data mode that is available for both the GIM and GEM science data is termed “raw mode”. When enabled, the 16- to 8-bit compression algorithm is turned off and the full resolution scaler numbers are inserted into telemetry instead of the compressed data. This has the effect of doubling the GIM and GEM science data rates but the small errors introduced by the compression algorithm are eliminated allowing detailed analysis of unaltered counts data should the need arise.

The Genesis Electron Monitor (GEM)

For the Genesis mission, it was decided to produce a copy the LANL BAM-E plasma electron experiment that is successfully being flown on the NASA/ESA Ulysses mission in order to minimize cost and reutilize a proven sensor design with extensive flight heritage. The reader is referred to Bame et al. (1983 and 1992) for detailed descriptions of the Ulysses electron sensor. The flight spare of the Ulysses instrument, with modified electronics, is also being successfully flown onboard the NASA ACE mission as the SWEPAM-E instrument (McComas et al., 1998). The sensor is somewhat oversized for the ~1 AU ACE and Genesis missions as it was originally designed to make electron measurements over the 1.3 – 5.0 AU range of the Ulysses orbit, but experience with the ACE instrument at L1 showed that no modifications to the design were necessary to meet Genesis performance requirements. The sensor portion of the GEM is therefore an almost

identical copy of the Ulysses and ACE instruments, while the electronics are of new design and have enhanced capabilities (Fig 11).

The GEM sensor basically consists of an ESA, for angle and energy analysis of incoming electrons, followed by a CEM detector array capable of single electron counting (Fig. 12). The ESA is a spherical-section analyzer with 120 deg bending angle, a 41.9 mm central radius and a nominal plate spacing of 3.5 mm (Table 1). The entrance aperture has dimensions of 3.5 x 10 mm. The plates are copper-coated and then blackened using the Ebanol-C process to suppress the number of unwanted UV photons that might reach the detectors and create a background. The analyzer plates are also scalloped perpendicular to the electron trajectories to further eliminate interferences from UV photons and photoelectrons generated in the ESA gap. The 1.22 mm radius grooves (3° period) have an amplitude of ~0.7 mm and reduce the ideal analyzer k factor from 6.0 to a calibrated value of 4.78. The 0 - 300 V range of the ESA HVPS and the ESA k factor set the energy GEM energy range of 0 to 1434 eV.

Electrons with appropriate entry angles and energies pass through the entrance aperture and ESA, and are then detected by one of the seven Galileo CEM detectors arrayed along the ESA exit gap. Energy scanning is accomplished by holding the outer ESA plate at ground potential while a positive bias on the inner ESA plate is stepped over the desired voltage range. A high-transmission (~90%) grid is located between the ESA exit and the front of the 10 mm diameter CEM funnels and is biased at +200 V to provide post-acceleration to the lowest-energy electrons, thereby increasing the efficiency with which they are counted. The CEM entrance funnels are held at the screen potential while the exit channel of the CEMs can be biased from 0 to +4000 V (+2700 V typical), necessitating a capacitive coupling of the output charge pulses to the Amptek A121 hybrid preamplifiers in the front-end electronics (FEE). The charge pulses are converted to digital signals that are accumulated in 16-bit scalars in the MEB until being read out to the S/C C&DH unit. CEM

gains are typically 6×10^7 at 2500 V and 3 kHz counting rate. The preamplifiers have a fixed deadtime of 0.5 μ sec.

The polar angular response of the GEM is ± 75 degrees with good overlap between the seven CEMs while the azimuthal angular acceptance varies from ± 5 degrees at 0 degrees polar angle to ± 14 degrees at 75 degrees polar angle (Fig. 13). The $\sim 10 \times 150$ degree acceptance fan is oriented such that the long dimension is parallel to the S/C spin axis and the center of the CEM #4 FOV looks along the equatorial plane of the S/C (i.e. the center of the GEM viewing fan is perpendicular to the S/C spin axis).

The GEM MEB is almost identical to that for the GIM with only a few exceptions (see Table 2 and MEB discussion above). The polarities of the CEM and ESA HVPSs are both positive and, due to the required resolution and dynamic range, the ESA stepping HVPS is a dual-range supply instead of the single-range type used in the GIM. Both ranges are 12-bit programmable with the low voltage range being variable from 0 to +6.39 V while the high range is commandable from 0 to +300 V. The internal microcontroller automatically handles the crossover between the ranges during energy scanning. Programming of the GEM microprocessor is also somewhat different to allow for a more relaxed data acquisition cadence and the simpler modes required for the electron sensor.

GEM Response and Calibration

The GEM response function was determined using a 2 keV ion beam (not an electron beam) and reverse biasing the ESA, i.e. negative potential was applied to the inner ESA plate to allow transmission of the ions through the analyzer. Normal biasing was used for the CEM detectors. The entrance aperture was illuminated with a uniform beam for all combinations of ESA potential, and azimuthal and polar angle to which the sensor was responsive. In this manner, a data cube of counts as a function of ESA voltage (equivalent to electron energy), polar angle and azimuthal angle was built up for each of the seven CEM detectors. The response function of the GEM can be completely determined using these

seven cubes. The relative responses of the GEM were calibrated to absolute beam flux using a solid-state detector with known output as a function of beam current.

Figure 14 shows the energy response of the GEM ESA, integrated over azimuth and polar angle. The individual CEM traces have been normalized to the maximum transmission observed for all CEMs. It can be seen that the energy resolution of the GEM ESA is ~13% FWHM but that the central energy of the response is shifted to somewhat lower values at the location of one of the highest polar angle detectors. This variation is unexpected and probably due to a minor misalignment of the ESA hemispheres and/or to drift of the beam energy during the course of the calibration run. The amplitude of the integrated transmission curves is expected to vary with the polar angle (i.e. CEM number) due to a decrease in apparent aperture area with increasing polar angle. This is complicated when integrated over azimuth angle due to a broadening of the azimuthal acceptance with increasing polar angle. Some variation in the height of the transmission curves is also probably due to variation of the individual CEM efficiencies and potential beam flux drift during calibration.

Figure 15 contains three plots of the GEM angular response. Fig. 15a is a plot of the “islands” of angular response integrated over energy, with each CEM island normalized to the maximum counts for that detector. The contours shown are for 90, 75, 50 and 25% response levels. It can be seen that there is good coverage of space by the viewing fan with an apparent broadening of the azimuthal response at high polar angles. The broadening effect is real and apparent when plotted in Cartesian coordinates, as done here. However, when these data are plotted using spherical-polar coordinates, the entire viewing fan appears to have similar azimuthal acceptance, independent of polar angle. The central response in the center of each of the islands can also be seen to describe a slight curve with polar angle, with highest polar angle detectors having the central response at more negative azimuths. This is a natural effect that arises from the practical necessity of having to offset

the sensor entrance aperture from the biased ESA plate to avoid electrical shorting (Gosling et al., 1978).

Figure 15b shows the GEM polar acceptance, integrated over energy and azimuth. The transmission values for the CEMs are normalized to the highest value observed for all detectors. The good overlap between the detectors at the ~50% level is apparent, as is the drop-off in transmission at high polar angles due to a cosine effect causing a decrease in apparent aperture area with increasing polar displacement. The response of the high polar angle detectors in this projection is higher than would be expected for a pure cosine drop-off because the response has been integrated over the expanded azimuthal transmission that can be seen in Figs. 15a and 15c. Polar angular resolution can be seen to be ~20 degrees FWHM, in good agreement with the calibration results of the ACE and Ulysses electron instruments (Bame et al, 1986 and 1992 and McComas et al, 1998). Transmission centers are within ± 1 degree of their design values.

The transmission of the GEM ESA is shown in Fig. 15c as a function of azimuthal angle, and is integrated over energy and polar angle. The individual response curves are all normalized to the highest value observed for all detectors. Here the transmission drop-off as a function of polar angle is more readily apparent (due to the projection) and the slight variation in central acceptance with polar angle is also visible. The integrated azimuthal resolution of the GEM can be seen to vary from ~12 degrees FWHM for the detectors at the lowest polar angles to 35 and 45 degrees FWHM at the highest.

GEM Operation

The operation of GEM is similar to but somewhat less elaborate than that of GIM. The basic Normal, Manual and Cal modes are almost identical to those discussed above for GIM but, as GEM continually scans a fixed, configurable energy range when in Normal mode, there is no need for the search cycles or the proton peak tracking employed by GIM. Initiation of data acquisition is identical to that for GIM: the S/C sends a Normal mode

acquisition command followed by a sync command to start data acquisition for each spin of the S/C.

Four spins of the S/C (~2.5 min.) are used by GEM to acquire a 3-dimensional measurement of the plasma electron distribution over ~96% of the 4 steradian unit sphere. A complete distribution measurement consists of counts collected from seven CEM detectors (polar angle) at twenty log-spaced ESA levels (energy) across twenty-four spin sectors (azimuthal angle). ESA voltage stepping is always from high energies to low energies. During the first spin of the four-spin data cycle, the highest five energies are scanned twenty four times, the second set of five energies are continuously scanned during the second spin, etc. until the data cycle is complete at the end of the fourth spin (Fig. 16). The period of each energy step in an energy scan is automatically adjusted to compensate for any variations in S/C spin rate. Nominal energy step times are 0.313 sec but these can vary by $\pm 10\%$ as spin rate increases or decreases during normal operations. Count integration times can be varied over a wide range to avoid counter spills or to improve counting statistics.

One of the main differences between GIM and GEM energy scanning is that the range covered by GEM is selected by command from the ground and remains fixed until the configuration is next changed. The measured energy range is easily configurable and can be set to cover any portion or all of the interval between 0 and ~1.4 keV, albeit with varying overlap of the energy response functions at the adjacent energy levels. The highest energy desired is selected and a step interval is set: this determines the amount in percent that each subsequent energy step should lay below the previous level. Typical values used are 287 V and 15.1%, which gives a scanned energy range of 61 to 1372 eV with good overlap of the energy response between levels. This energy interval avoids the photoelectron distribution and gives good coverage of the energy interval where counter-streaming electron distributions are typically found.

GEM Data

As opposed to the case for GIM, all of the GEM counts data are sent to the ground for analysis, i.e. there is no masking of the GEM data as is the case for the GIM (see masking discussion above). The 3,360 16-bit scaler values for a complete data cycle are all read out from the GEM MEB to the C&DH unit, compressed to 8-bit numbers and inserted into the telemetry stream. The compression algorithm introduces a maximum error of ~3% in the counts data. The effective science data rate of the GEM is reduced from ~358 bps to ~179 bps (only marginally higher than the 169 bps GIM data rate) by use of the compression scheme. The uncompressed data is used on-board by the WIND algorithm to determine the presence of bi-directional electron streams (BDES) but is first corrected for electronic deadtime and detector background. The background correction involves an algorithm that averages the counts data from all seven CEMs at the highest energy level and at all twenty four azimuths to arrive at an average background counts correction. If the average is <10 counts, no correction is made. For a background count average between 10 and 500, the correction is subtracted from each data element before further processing. If the average exceeds 500 counts (background count rate ~2.5 kHz) the GEM data are marked false and BDES processing is suspended until background rates subside.

Monitor Simulators and System Level Testing

Realistic end-to-end testing of integrated payload components is an important aspect of any S/C test plan. This is even more important for Genesis as GIM and GEM provide raw plasma counts data to the S/C C&DH subsystem, which then processes the data into moments, makes solar wind regime determinations, and appropriately controls the Concentrator and Collector Arrays, all via the WIND algorithm. But complete end-to-end testing was not strictly possible due to an inability to realistically simulate the solar wind

environment at the S/C testing level. To still allow nearly end-to-end testing, a system was devised in which raw data from GIM and GEM were simulated and injected into the spacecraft C&DH for testing of the remainder of the system, including autonomous commanding of the collector arrays when the simulated data indicated a change in solar-wind regime. The spacecraft ability to telemeter these regime changes and array motions to a ground station were also tested. The only portion that was not truly end-to-end was the fact that GIM and GEM had to be tested separately with ion and electron beams in a vacuum chamber off-line.

The near-end-to-end simulation tests followed a several-step process as follows. Solar-wind ion data recorded for various time periods by the ACE SWEPAM-I instrument, often modified to test a particular portion of the WIND algorithm, were used for the simulation tests. The data were input as ground-processed moments into the GENSIM program that takes ACE moments and converts these data into raw counts data anticipated for GIM, reversing the process that normally produces moments from raw counts. For the GEM data, a simple bi-directional-electron index was assigned for each data cycle. These simulated counts were then input from PCs into GIM and GEM electronic simulator boxes. The simulator boxes look identical to the actual GIM and GEM instruments to the spacecraft from an electronic and signal-processing standpoint. The simulator boxes were used both for initial safe-to-mate tests (they were available for these tests long before the actual instruments were ready) and for the simulations. The simulator boxes produced data packets simulating in-flight GIM and GEM data, which were fed to the spacecraft C&DH. The C&DH in turn processed the data packets using the WIND algorithm described in Neugebauer et al. (this issue) and made solar-wind regime selections accordingly.

The simulation scheme was first used to extensively test the WIND algorithm in the Software Test Laboratory (STL), which simulated the spacecraft C&DH and its environment. A number of tests were devised, as listed in Table 3, to test various solar-wind regime transitions, and various other features such as shock detection, despiking of noisy

data, dropout of various types of data under abnormal solar-wind conditions, and turning the concentrator voltages to standby for excessively high wind speeds.

The STL tests were performed over a period of nearly one year prior to launch of the spacecraft. Overall they were very useful in debugging the moments extractor code, which processed the raw data, and the WIND algorithm, which selected the solar-wind regime. Only one of these tests was performed on the spacecraft, on two different occasions, to test the near-end-to-end performance, including moving the collector arrays.

Performance in flight proved the success of these tests, as only one surprise was found in the code in flight, and that was in the BDEs section, which was not as well tested by this scheme (Neugebauer et al., 2002).

Initial Results

GEM began making solar wind measurements on Aug. 23, 2001 and GIM was turned on for the first time the following day. As of April 2002, only a few days of measurement time have been lost due to S/C safe-mode entry, trajectory correction maneuvers, S/C reconfiguration, etc. and no anomalies have been noted in the instrument operation. The level of solar activity since turn-on has been relatively high with the S/C having already encountered a number of solar energetic particle events, some with very high particle flux levels. As expected, instrument backgrounds generated by penetrating radiation have been considerably higher in GEM than in GIM as 1) detector biasing in GEM attracts the numerous secondary electrons produced by energetic particles in the sensor interior and 2) the GEM wall thicknesses are considerably less than for GIM, thereby allowing easier penetration of energetic species. No unwanted backgrounds from direct solar UV light leaks, or from internal UV-generated secondary electrons, have been observed in either GIM or GEM while the S/C is in normal orientation.

Figure 17 shows a color-coded, polar plot of GIM counts obtained shortly after instrument turn-on when Diagnostic mode data was available. Each of the eight rings represents one of the CEM detectors with the central disk showing CEM#1, which is looking along the S/C spin axis into the nominal solar wind direction. Angle around the plot represents azimuthal look direction (there are forty azimuthal samples around each ring) and increasing radial distance from the center is equivalent to increasing polar angle from the spin axis. Each ring is ~3 degrees in width. A normal to the center of the plot points in the direction of the Sun and lies in the ecliptic. The area shown can be thought of as a circular FOV of the sky with half-angle of ~25 degrees, centered ~ 4.5 degrees west of the center of the Sun. Counts have been integrated over all energies.

It can be seen that the solar wind is fairly well centered in CEM #1 and that the beam is rather cool as counts drop off very sharply with polar angle from the center of the FOV. There is a slight displacement of the flow toward the upper right of the plot as is evidenced by a small modulation in the counts most easily seen in CEMs #3 and #4. The high degree of oversampling in the center of the plot can easily be seen and serves to illustrate why the data masking scheme can be employed to greatly reduce telemetry while having little effect on angular resolution. Subsequent analysis of the solar wind data indicates that the flow speed during this period was ~360 km/sec, density was ~0.9 cm⁻³, and proton temperature was ~8.9 x 10⁴ K.

To illustrate the energy resolution of the GIM, four spectra are plotted in Figure 18. Each energy spectrum was acquired over one 2.5-minute data cycle, is constructed of raw counts sampled over 40 msec by the detector with the maximum counts at forty different energies, and is integrated over azimuthal angle. Fig. 18a shows a slow solar wind flow with a typical proton temperature ($V_p=361$ km/s, $T_p=6.0 \times 10^4$), Fig. 18b is a fast stream with a typical temperature ($V_p=679$ km/s, $T_p=3.4 \times 10^5$), Fig. 18c shows a CME flow with low temperature and high alpha abundance ($V_p=354$ km/s, $T_p=6.0 \times 10^4$, [He]=13%) and Fig. 18d was obtained from the compressed solar wind at the leading edge of a solar wind

stream that has higher than typical temperature ($V_p=520$ km/s, $T_p=3.9 \times 10^5$). These figures serve to illustrate that the track energy range of the GIM is adequate to cover the proton and alpha peaks for almost any solar wind condition that will be encountered, that the very good energy resolution can easily resolve the proton and alpha peaks except at the hottest temperatures where the distributions become inextricably overlapped in e/q , and that the peak resolution is more than adequate for determining good plasma moments. The reader is referred to the companion paper by Neugebauer et al. (this issue), which gives the details of how the GIM counts spectra such as these are converted on-board to plasma moments and how these moments are used to make real-time adjustments of the collector subsystems. Several examples of moments time-histories derived from GIM flight data are also presented.

Figure 19 illustrates the ability of the GEM to meet its requirements of being able to determine the presence/absence of bi-directional electron streaming. This parameter is one of those used in the real-time identification of CME flow past the S/C. Figure 19a is a series of nine energy-cuts (of twenty available) showing the location in polar and azimuth angle of the solar wind electron strahl. Note that only a single beam is evident, centered at ~ 70 degrees polar and 100 degrees azimuth angle, but it is clearly visible over the range of at least 200 to 1000 eV.

Figure 19b is an identical series of nine energy-cuts taken ~ 25 hr. after 19a but a counter-streaming beam, located ~ 180 degrees opposite the antisunward-strahl, is now clearly visible. Such bi-directional electron streams can sometimes be encountered in CMEs when regions with closed magnetic field lines transit the S/C. The WIND algorithm checks that at least three energy levels in the appropriate energy range contain significant evidence of counter-streaming electrons before declaring their presence valid.

Conclusions

The GIM and GEM are currently providing fully 3-dimensional measurements of the solar wind ion and electron populations at L1 in support of the primary operational goal of the Genesis mission, namely, the collection of ultrapure solar wind samples for return to Earth. Additionally, the Genesis solar wind data set is quite useful in itself for numerous heliospheric studies, but is somewhat limited due to the lack of magnetic field and energetic particle data. The real value of the Genesis solar wind measurements may be when used in combination with data sets from other spacecraft located L1 (e.g. ACE, WIND, SOHO) and elsewhere (Ulysses) for multi-spacecraft studies of large-scale phenomena in the solar wind.

Acknowledgements

Work at Los Alamos was performed under the auspices of the U.S. Dept. of Energy with financial support from the NASA Genesis mission. A large number of highly talented individuals at LANL, SwRI, LMA and JPL were involved in making the GEM and GIM instruments a reality and we gratefully acknowledge their invaluable contributions.

References

Bame, S.J., Glore, J.P., McComas, D.J., Moore, K.R., Chavez, J.C., Ellis, T.J., Peterson, G.R., Temple, J.H., and Wymer, F.J.: 1983, 'The ISPM solar wind plasma experiment', The International Solar Polar Mission – Its Scientific Investigations, ESA SP-1050, 47.

Bame, S.J., McComas, D.J., Barraclough, B.L., Phillips, J.L., Sofaly, K.J., Chavez, J.C., Goldsteinn, B.E. and Sakurai, R.K.: 1992, 'The Ulysses solar wind plasma experiment', *Astron. Astrophys. Suppl. Ser.*, 92, 237.

Burnett, D.S., Barraclough, B.L., Bremmer, R.R., Neugebauer, M., Oldham, L.P., Sasaki, C.N., Sevilla, D., Smith, N., Sansbery, E., Sweetnam, D., and Wiens, R.C.: 2002, 'The Genesis Discovery mission: return of solar matter to Earth', *Space Sci. Rev.*, this issue.

Gosling, J.T., Asbridge, J.R., Bame, S.J., and Feldman, W.C., 1978, 'Effects of a long entrance aperture upon the azimuthal response of spherical section electrostatic analyzers', *Rev. Sci. Instrum.*, 49(9), 1260.

Jurewicz A.J.G., Burnett D.S., Wiens R.C., Friedmann T.A., Hays C.C., Hohlfelder R.J., Nishiizumi K., Stone J.A., Woolum D.S., Becker R., Butterworth A.L., Campbell A.J., Ebihara M., Franchi I.A., Heber V., Hohenberg C.M., Humayun M., McKeegan K.D., McNamara K., Meshik A., Pepin R.O., Schlutter D., Wieler R.:2002, 'Overview of the Genesis solar-wind collector materials', *Space Sci. Rev.*, this issue.

McComas, D.J., Bame, S.J., Barker, P., Feldman, W.C., Phillips, J.L., and Riley, P.:1998, 'Solar wind electron proton alpha monitor (SWEPAM) for the Advanced Composition Explorer', *Space Sci. Rev.*, 86, 563.

Neugebauer, M., Steinberg, J.T., Tokar, R.L., Barraclough, B.L., Dors, E.E., Wiens, R.C., Gingerich, D.E., Luckey, D. and Whiteaker, D.B.: 2002, 'Genesis on-board determination of the solar wind flow regime', *Space Sci. Rev.*, this issue.

Nordholt J.E., Wiens R.C., Abeyta R.A., Baldonado J.R., Burnett D.S., Casey P., Everett D.T., Lockhart W., McComas D.J., Mietz D.E., MacNeal P., Mireles V., Moses R.W. Jr., Neugebauer M., Poths J., Reisenfeld D.B., Storms S.A., and Urdiales C.: 2002, 'The Genesis Solar Wind Concentrator', *Space Sci. Rev.*, this issue.

Wiens R.C., Neugebauer M., Reisenfeld D.B., Moses R.W. Jr., and Nordholt J.E.: 2002, 'Genesis solar wind concentrator: Computer simulations of performance under solar wind conditions', *Space Sci. Rev.*, this issue.

Table 1 – GIM and GEM Instrument Parameters

	<u>GEM</u>	<u>GIM</u>
Species Measured	Electrons	Ions
Number of CEM Detectors	7	8
Energy Resolution (% FWHM)	13	5.2
Azimuthal Resolution (deg FWHM) (* function of polar angle)	12* - 40*	4.2
Polar Resolution (deg FWHM)	20	3.0
Polar FOV (deg)	150	26
Center of Sensor FOV	90° from S/C spin axis	10.5° from S/C spin axis
ESA Central Radius (mm)	41.9	60.0
ESA Bending Angle (deg.)	120	120
ESA Gap (mm)	3.5	1.8
k-factor (accepted energy/ESA voltage)	4.7	14.7
Aperture Length along plates (mm)	10.0	2.90
Energy Range (eV/q)	1-1,430	1-13,600
Time per Spectrum (min)	2.5	2.5
Mass (kg)	2.2	2.6
Power (watts)	3.67 peak 3.55 average 3.0 HVPS off	3.91 peak 3.8 average 3.0 HVPS off
Base dimensions (inches)	6.5 x 8.5	6.5 x 8.5
Telemetry rate (bps effective)	179	169

**Table 2 - Monitor Electronics Box (MEB)
Output Voltages**

	CEM HVPS	ESA HVPS	Discriminator Threshold
GIM	0 to -4.0 kV	0 to -925 V	0 to +5 V
Accuracy (whichever greater)	$\pm 1\%$ or 3 V	$\pm 1\%$ or 0.5 V	$\pm 1\%$
GEM	0 to +4.0 kV	0 to +300 V	0 to +5 V
Accuracy (whichever greater)	$\pm 1\%$ or 3 V	$\pm 1\%$ or 0.25 V	$\pm 1\%$

Table 3 - Solar-wind simulation tests used to verify correct on-board processing of the raw GIM and GEM data and correct performance of the WIND algorithm (Neugebauer et al., 2002).

Test	Description
F1	Despiking of data
F2	Test for proper performance during alpha data drop-out
T1	Fast to slow wind regime transition
T2	Fast to CME wind regime transition
T3	Slow to fast wind regime transition
T4	Slow to CME wind regime transition
T5	CME to fast wind regime transition and concentrator-to-standby test
T6	CME to slow wind regime transition
24 hr test	Long-duration run to test features having longer time constants
50 hr test	Long-duration run performed in STL shortly before launch

Figure Captions

Figure 1 – The Genesis spacecraft in solar wind collection configuration showing the location of the GEM. The GIM location is directly opposite the GEM but is hidden in this view by the Sample Return Capsule. All sample collection materials are located in the Science Canister.

Figure 2 – Layout of the Genesis equipment deck with the Sample Return Capsule removed and the locations of the GEM and GIM indicated. The GEM viewing fan is directed radially outward from the center of the deck while the GIM fan is oriented upward, with one edge of the fan lying parallel to the +X axis.

Figure 3 – Simplified schematic view of the GIM sensor showing the ESA and the CEM array positioned behind the analyzer exit gap. The FOV of the individual detectors is also indicated. The analyzer is mounted such that the center of the FOV of CEM#1 is aligned with the spacecraft spin axis

Figure 4 – Photo of the GIM just prior to final preparations for delivery to the spacecraft. A wedge containing the FEE tilts the hermetically-sealed sensor “coffin” 10.5 degrees from the vertical to orient the FOV along the spacecraft spin axis. A deployable door covers the ESA entrance aperture that is located in the center of the four MLI-interface posts visible on the top of the sensor. The MEB containing the HVPS and Controller boards is the box at the bottom of the stack. Dimensions of the base are 21.6 x 16.5 cm (8.5 x 6.5 inches).

Figure 5 – Drawing showing the ~4 x 25 degree GIM viewing fan and the individual CEM viewing angles. During spacecraft rotation, the fan sweeps out a circle on the sky with ~50 degree diameter.

Figure 6 – GIM response to a 5 keV ion beam as a function of ESA voltage (equivalent to ion e/q). Response has been integrated over polar and azimuth angle and normalized to the maximum number of counts observed. The FWHM energy response can be seen to be ~5.2% and varies slightly with CEM.

Figure 7 – Calibration of GIM angular response. 7a – Map of CEM response islands integrated over energy. Contour intervals represent 90, 75, 50 and 25% response levels for the individual detectors. 7b – Polar response of the detectors integrated over azimuth and energy. Response curves are normalized to the maximum counts for all detectors. 7c – Azimuthal response of the GIM integrated over polar angle and energy. Responses are normalized to the maximum observed.

Figure 8 – Schematic of a four-spin GIM Normal mode data acquisition cycle. Scheme is essentially identical for GEM except that there are five energy steps per spin sector and twenty four spin sectors per spin of the S/C.

Figure 9 – Schematic of the individual energy steps in a typical energy sweep. Scheme is applicable for both GIM and GEM except that different times are used for each instrument.

Figure 10 – Mask scheme used to accommodate oversampling and reduce GIM telemetry rate. Pluses are acquired samples and diamonds are samples selected for downlink. Figure 10a – Example of mask used when solar wind beam is located near the S/C spin axis.

Figure 10b – Example of mask used when solar wind beam is located ~7 degree off-axis.

Figure 11 – Photo of GEM during final preparations before delivery to the S/C. The round drum is the hermetically-sealed sensor head and is essentially identical to those used for

ACE and Ulysses. The electron entrance aperture is located beneath the deployable door in the center of the square MLI-interface bracket on the front of the drum. The MEB base dimensions are 6.6 x 8.5 inches.

Figure 12 – Simplified schematic of the GEM taken from Bame et al., 1983. The back and cross-sectional views show the ESA and the CEM array positioned behind the analyzer exit gap. The spin axis and the viewing fan are indicated. The spin axis is out of the paper in the cross-sectional view.

Figure 13 – Mechanical drawing of the GEM showing the overall viewing fan and the look directions for each of the CEMs.

Figure 14 – Energy response of the GEM ESA integrated over polar and azimuth angle. The response curves give an energy resolution of ~13% FWHM. A 2 keV ion beam was used for the calibration.

Figure 15 – Calibrated angular response of the GEM. Figure 15a – Map of the transmission islands integrated over energy. The contours show 90, 75, 50 and 25% transmission levels for each detector. Figure 15b – Polar angular response for each of the detectors integrated over azimuth and energy. The response curves have been normalized to the maximum transmission for all detectors. Figure 15c – Azimuthal angular response integrated over polar angle and energy. The detector transmissions have been normalized to the maximum observed for all detectors.

Figure 16 – Schematic of a four-spin GEM Normal mode data acquisition cycle. The length of the energy steps and hence a complete data sweep expands and contracts as S/C spin rate varies.

Figure 17 – A polar plot centered on the average solar wind direction at L1 using Diagnostic mode data and demonstrating angular resolution of the GIM. The plot can be thought of as a view of the sky with radius of ~25 degrees and polar resolution of ~3 degrees in each ring and forty samples of azimuthal resolution. The oversampling near the center of the FOV is evident.

Figure 18 – GIM ion energy spectra from four separate periods illustrating the energy resolution of the instrument. Spectra are from the single detector with the maximum counts and are integrated over azimuth. See text for an explanation of the solar wind conditions extant for each spectrum.

Figure 19 – Two GEM angle-angle plots showing 19a) a typical antisunward solar wind electron strahl and 19b) an antisunward as well as a sunward strahl more commonly referred to as a bidirectional electron stream, often indicative of a coronal mass ejection. The numbers in the left margin of each snapshot give the electron energy sampled while those in the right margin give the maximum and minimum number of counts observed at that energy. The color scale in each frame is normalized to the maximum number of counts seen in that frame.

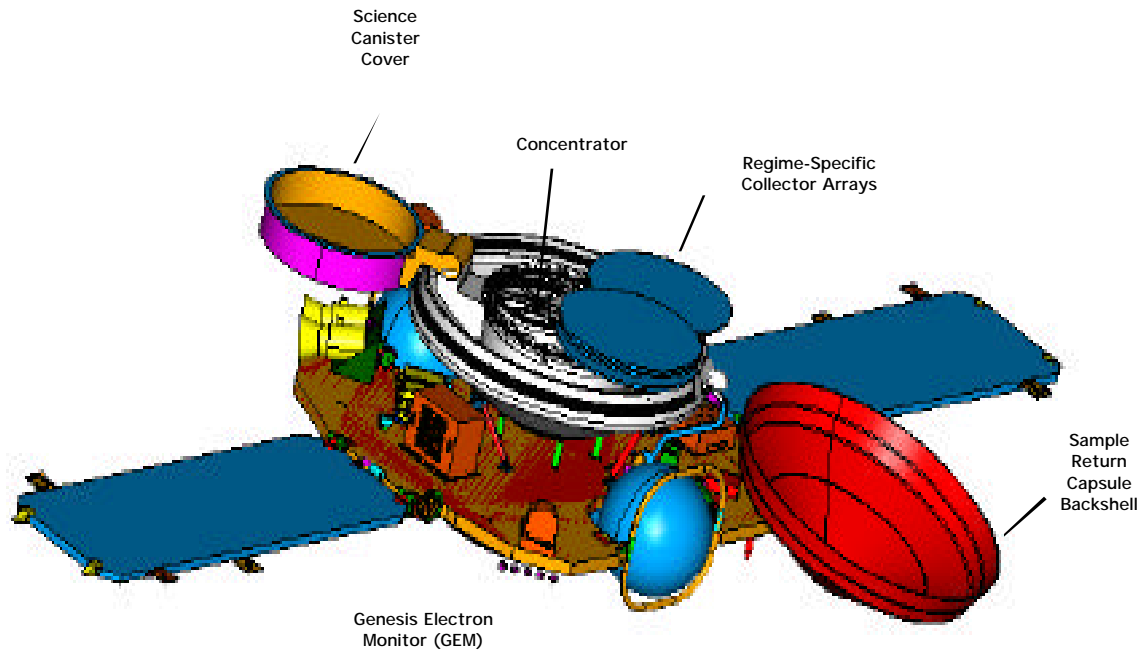


Figure 1

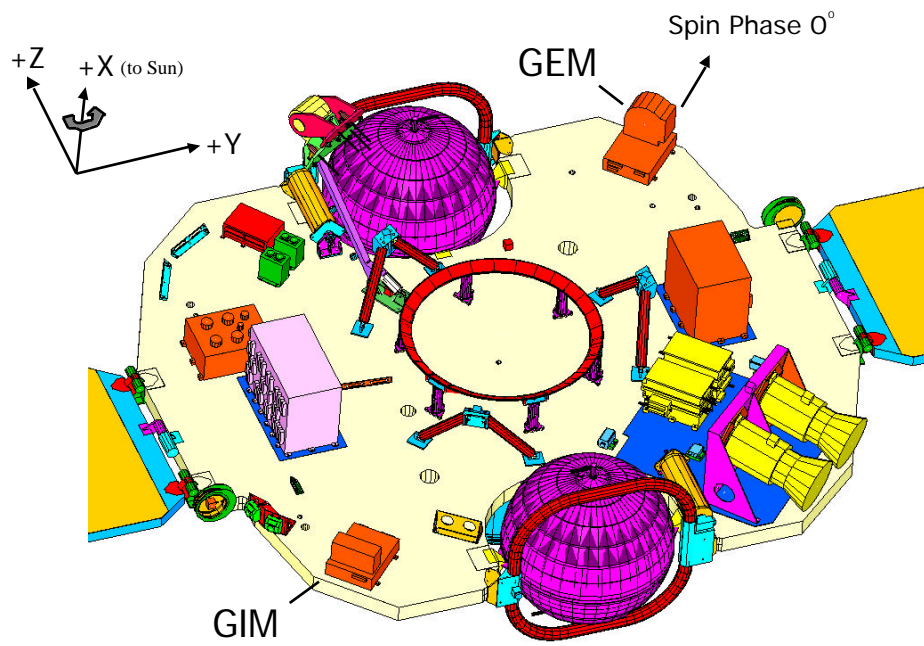


Figure 2

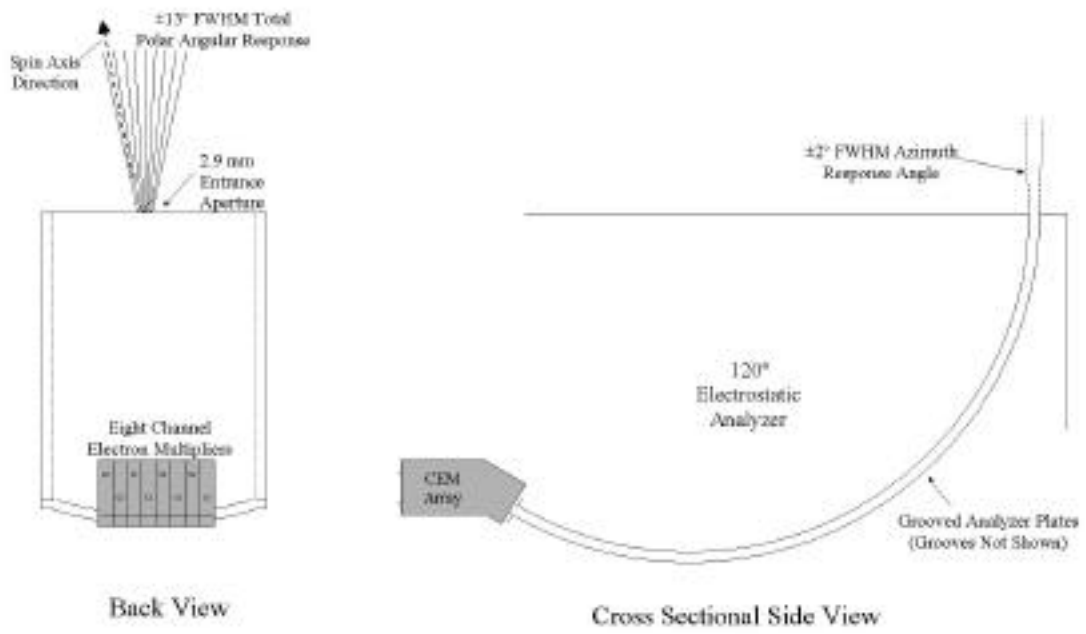


Figure 3

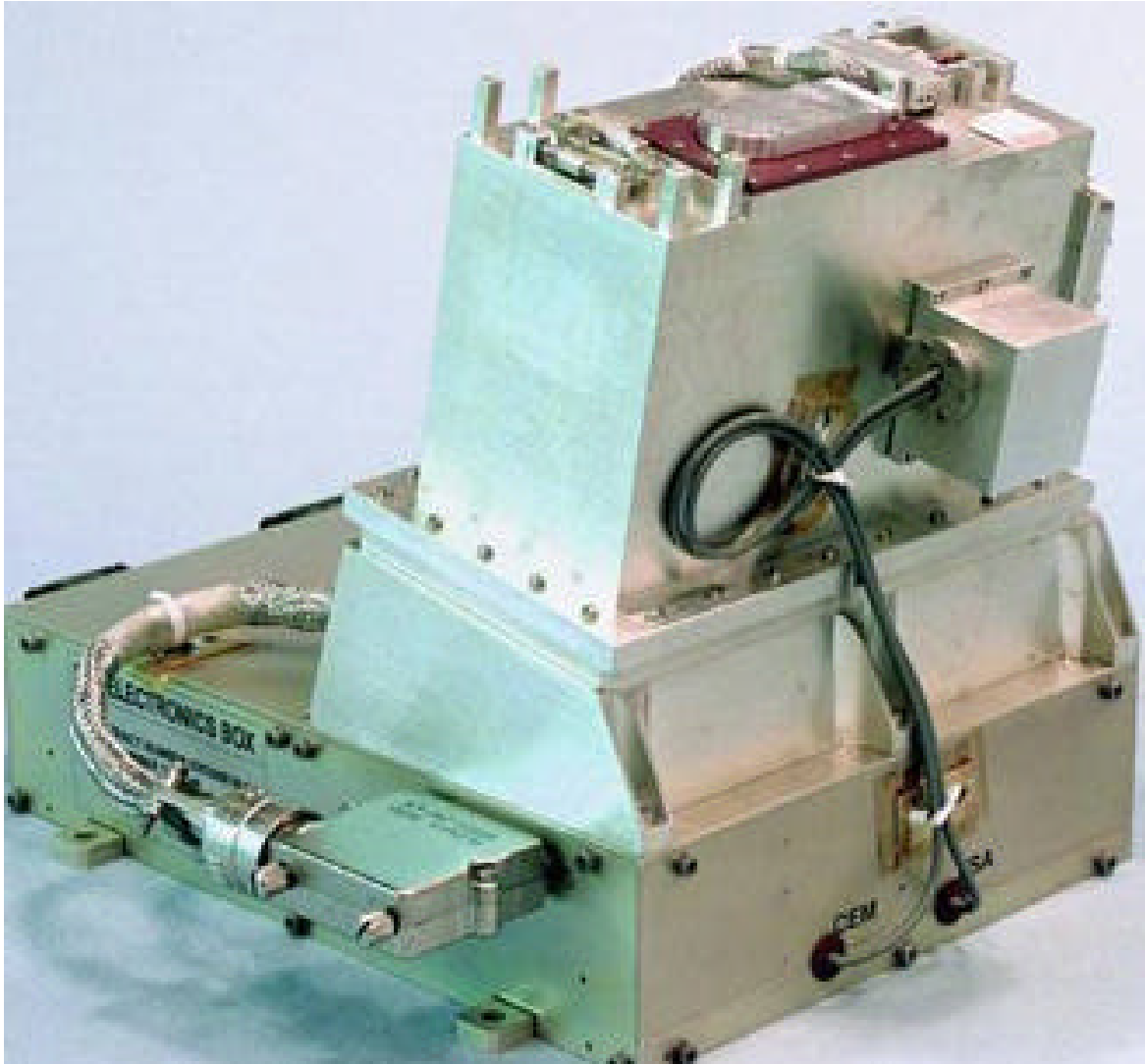


Figure 4

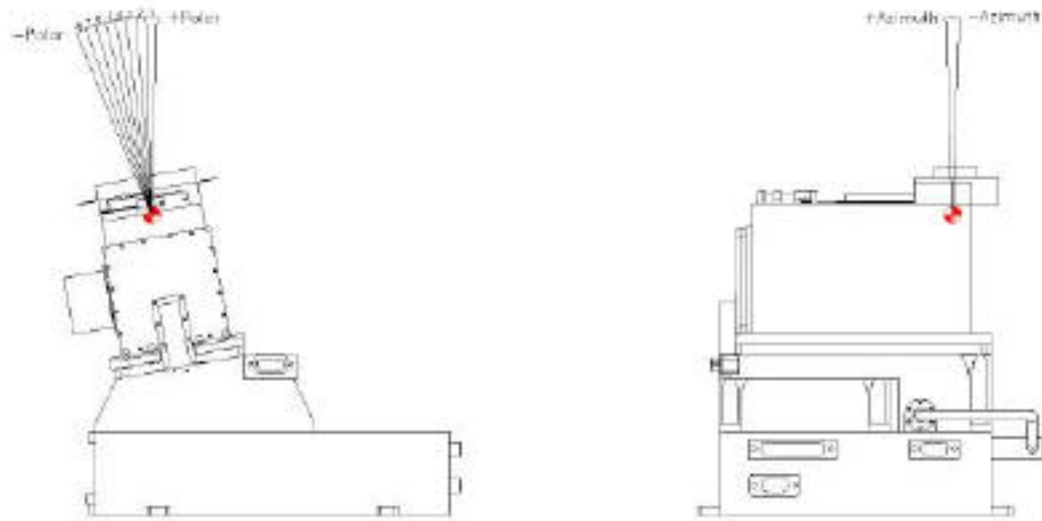


Figure 5

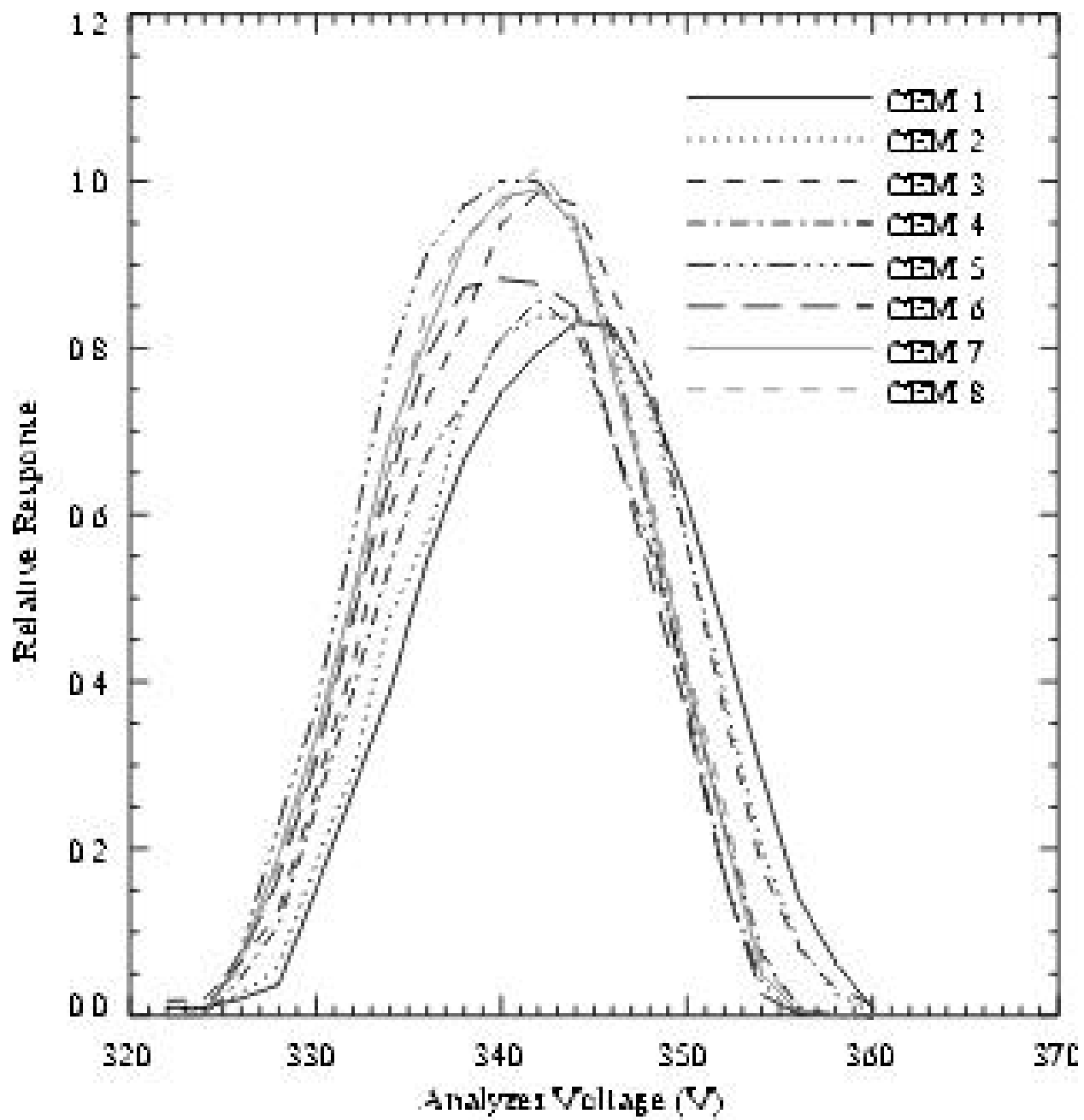


Figure 6

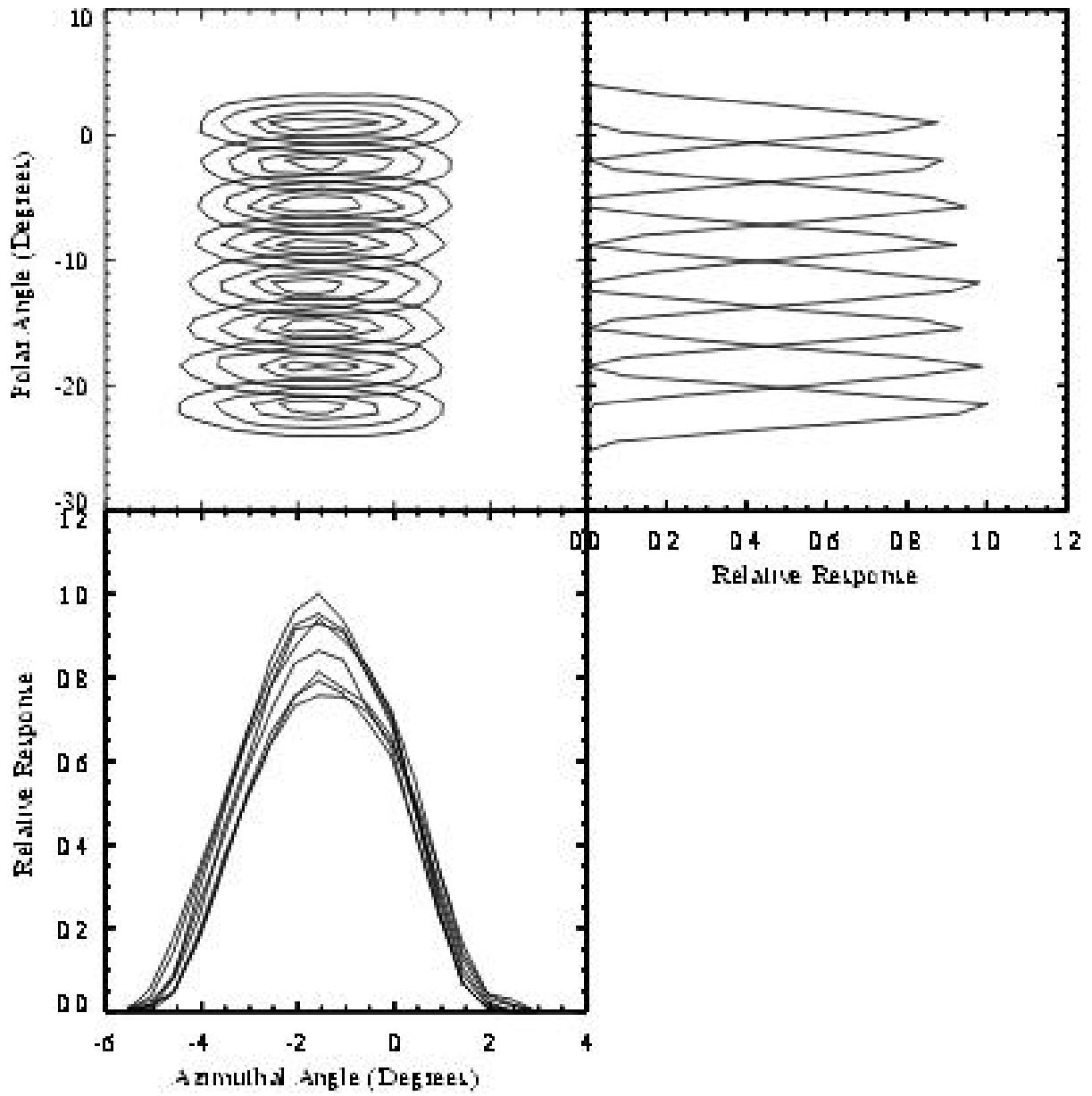


Figure 7 a,b,c

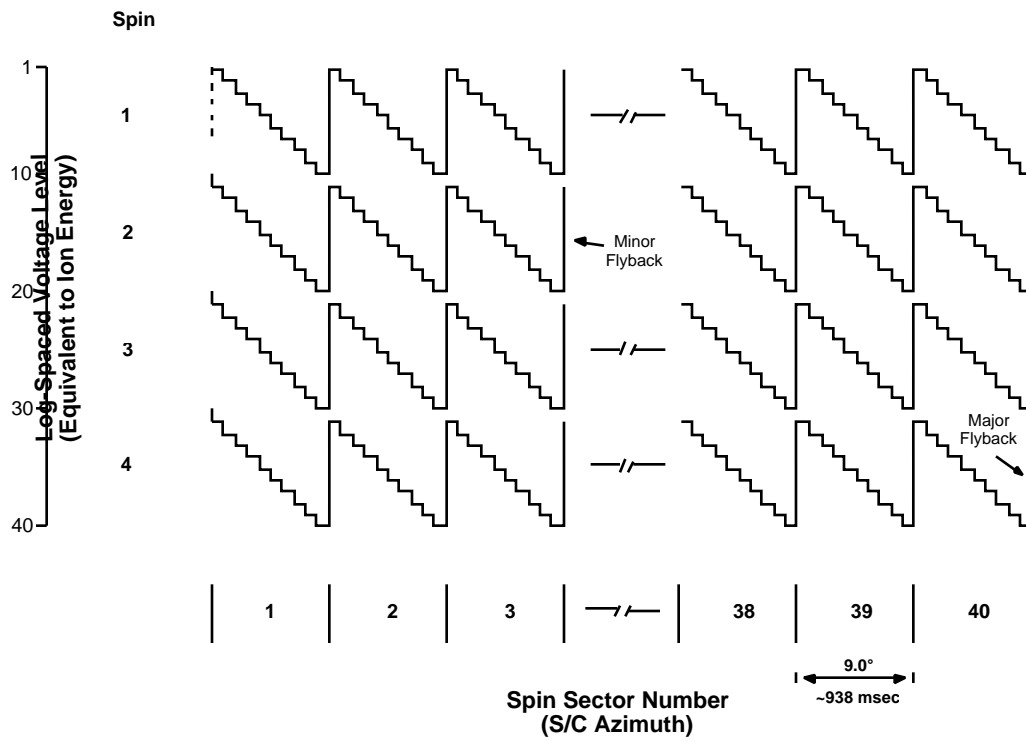


Figure 8

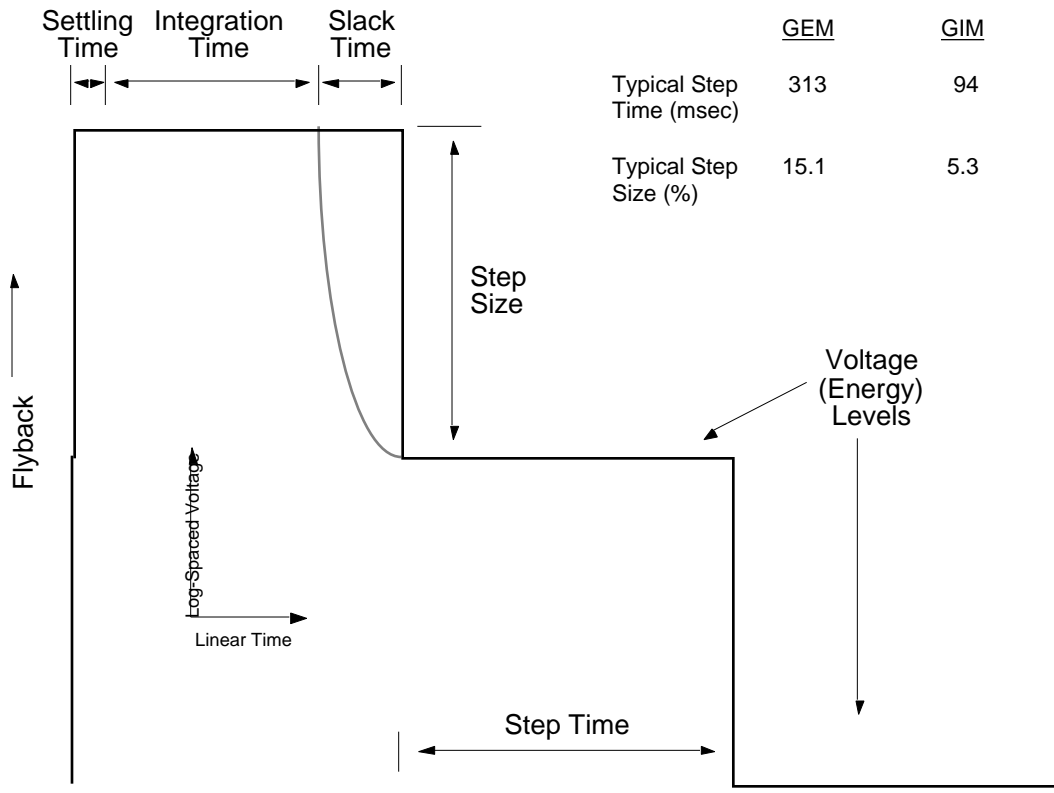


Figure 9

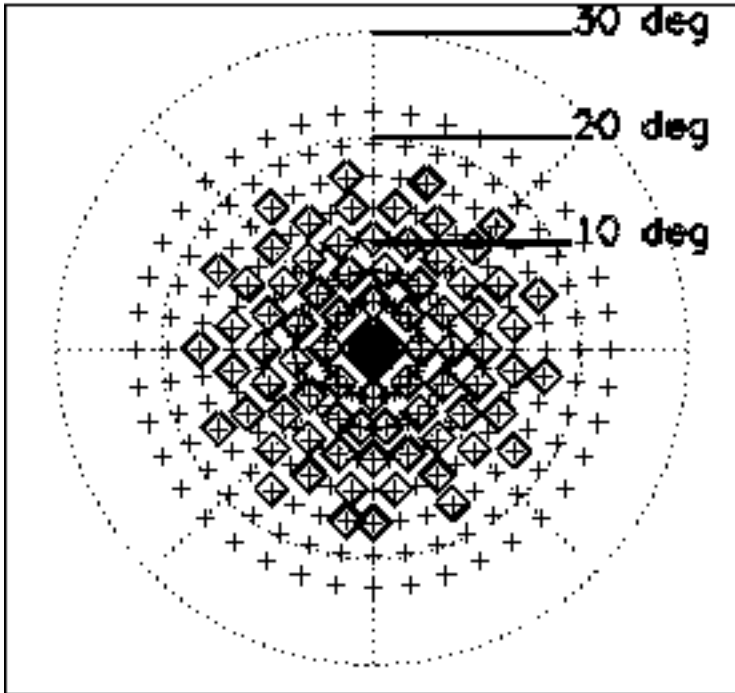


Figure 10a

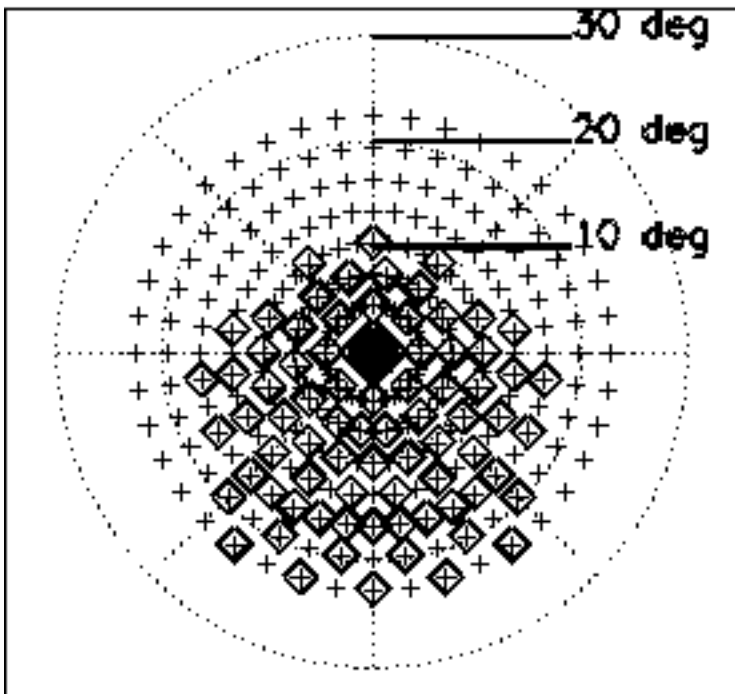


Figure 10b

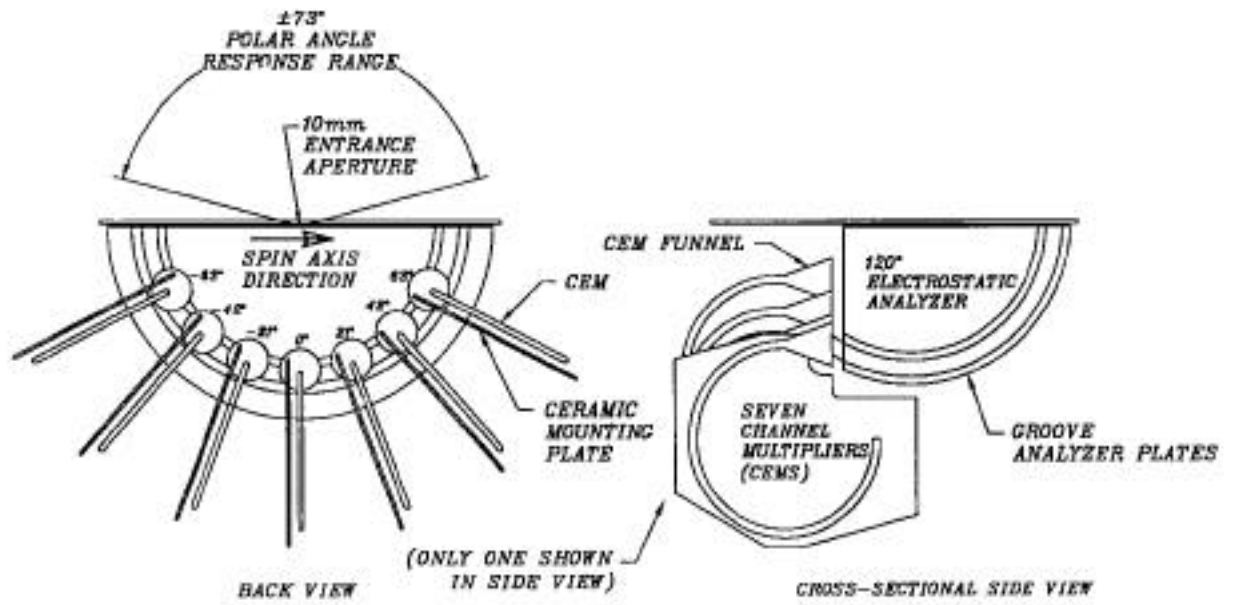


Figure 12

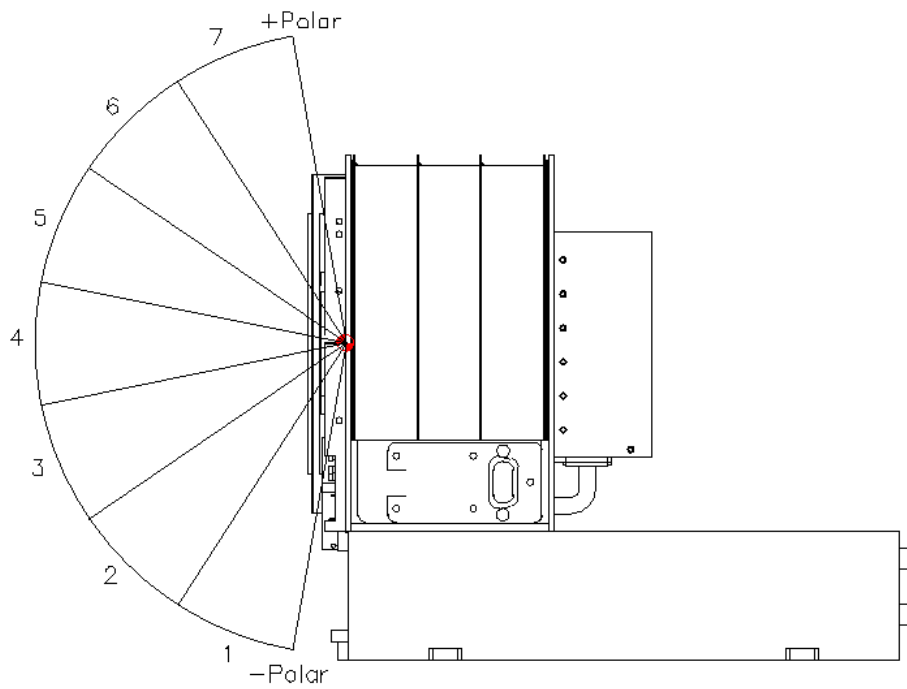
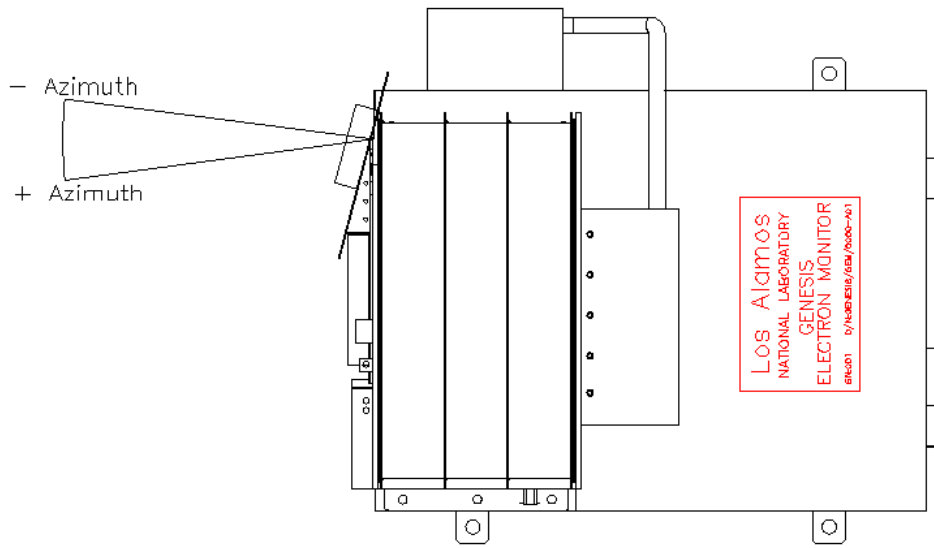


Figure 13

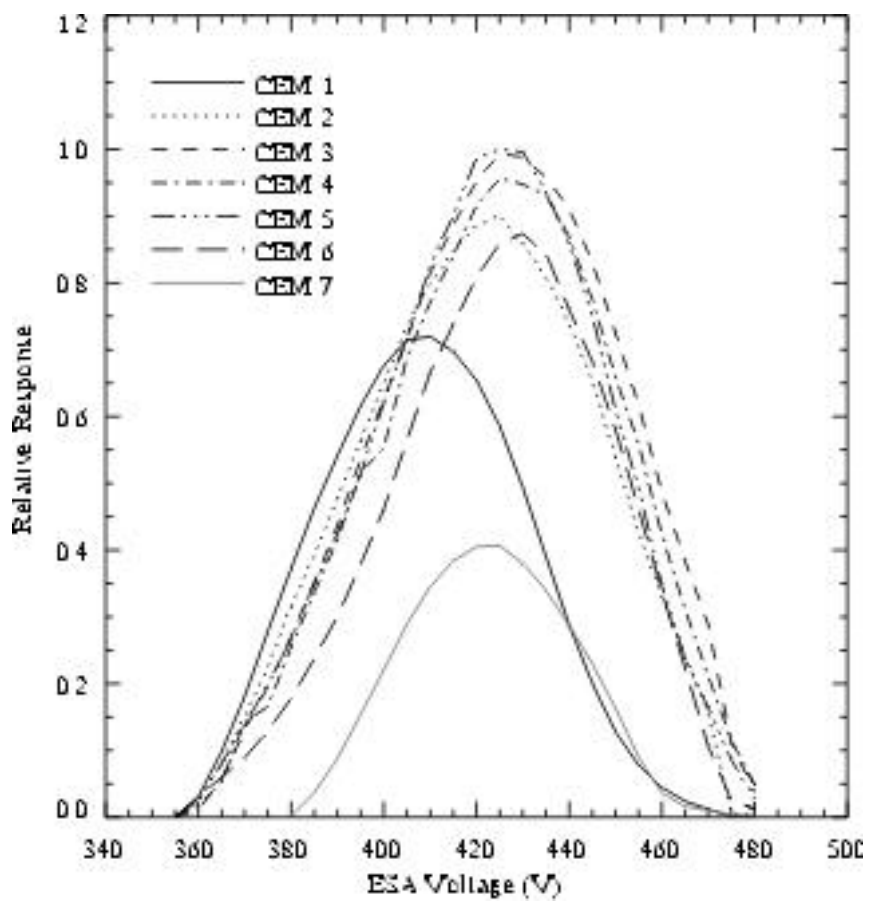


Figure 14

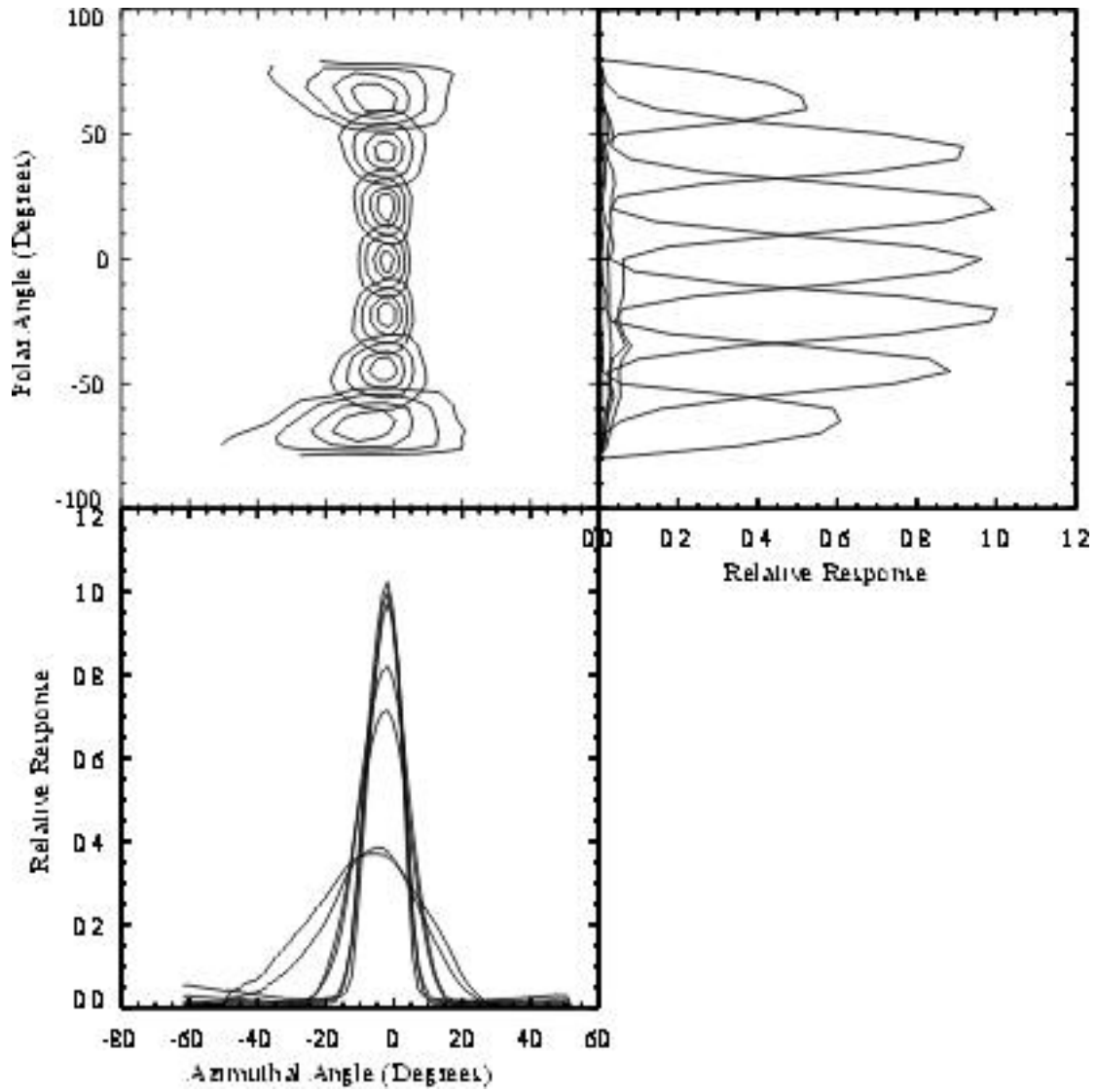


Figure 15

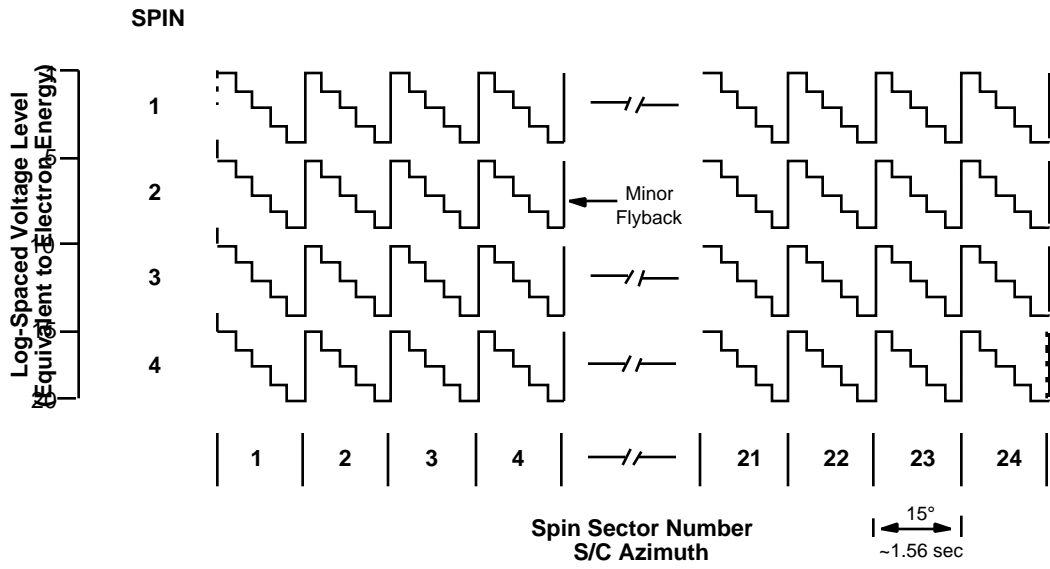


Figure 16

Genesis/GM: summed COUNTS: 2001 AUG 24 16:45:29 [Diag mode]

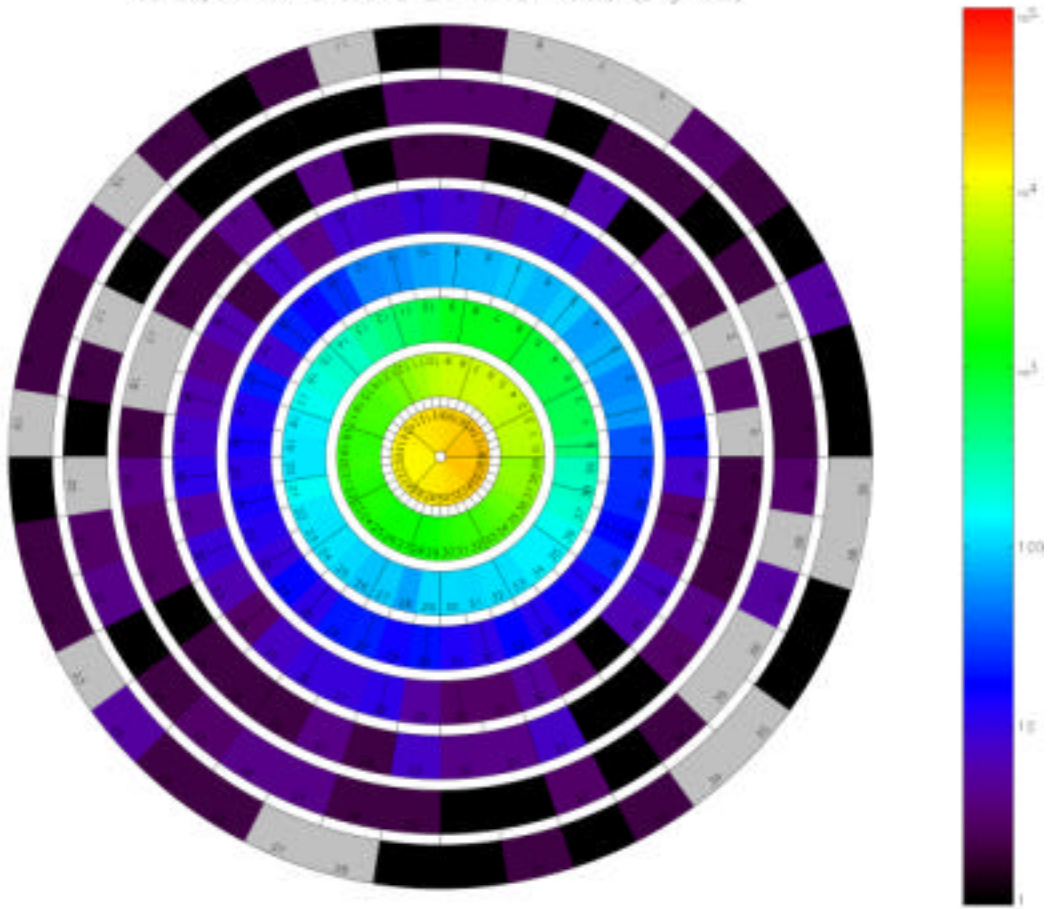


Figure 17

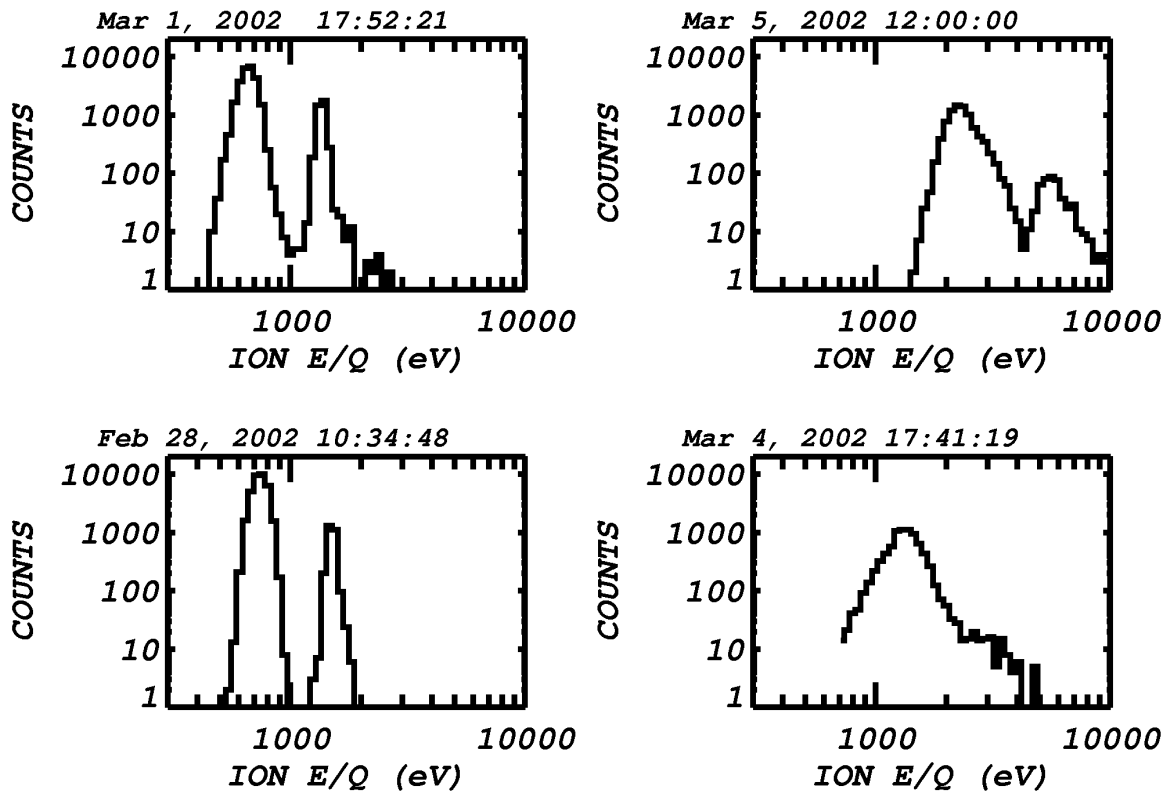


Figure 18

GENESIS ELECTRON MONITOR 2001 OCT 21 11:21:38

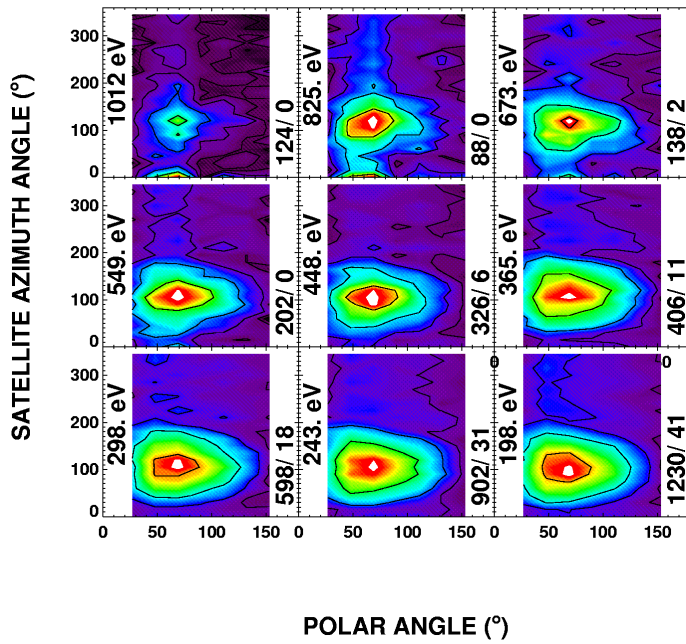


Figure 19a

GENESIS ELECTRON MONITOR 2001 OCT 22 12:47:36

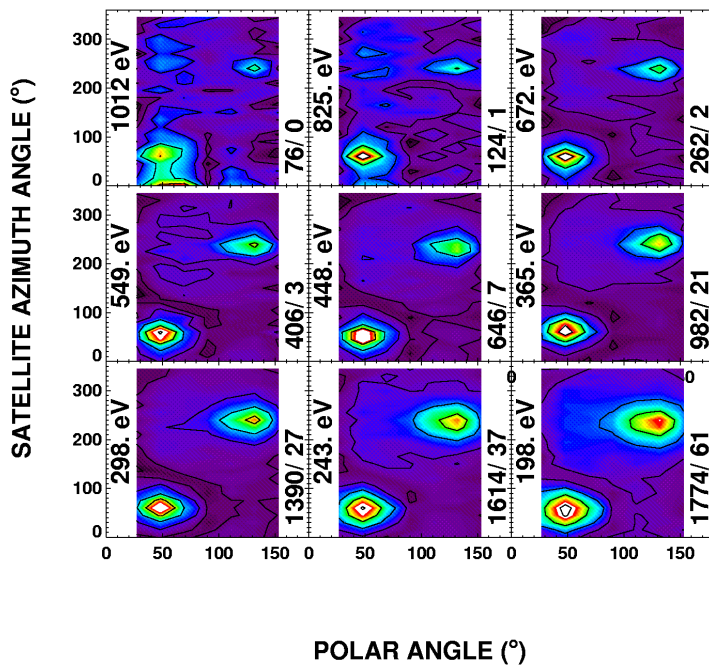


Figure 19b